Abstracts From the Pulmonary Pathology Society 2019 Biennial Meeting

Presented here are the scientific abstracts from the Pulmonary Pathology Society (PPS) Biennial Meeting, which took place in June 2019 in Dubrovnik, Croatia. This meeting of pulmonary pathologists from around the world was assembled under the direction and leadership of Mary Beth Beasley, MD, then president of the PPS. All abstracts were reviewed for scientific content by Mari Mino-Kenudson, MD, and Andre Moreira, MD, prior to their acceptance.

Genotype Mutations and Immune Cell Phenotypes Modulate Metastases and Prognosis in Non–Small Cell Lung Carcinomas

V. Capelozzi[1]; J. Rugolo-Machado[2]; A. Fabro[3]; C. Farhat[3]; E. Parra.[4]
[1]Department of Pathology, University of São Paulo Medical School, São Paulo, Brazil; [2]Clinicas Hospital, Faculty of Medicine, State University of São Paulo, Botucatu, Brazil; [3]Department of Pathology and Legal Medicine, Ribeirão Preto School of Medicine, University of São Paulo, Ribeirão Preto, Brazil; [4]Department of Translational Molecular Pathology, The University of Texas MD Anderson Cancer Center, Houston.

Context: To gain insight into the pathogenesis and progression of non–small cell lung carcinomas (NSCLCs) by (1) characterizing the tumor microenvironment using multiplex immunofluorescence, image analysis, and genetic mutation analysis and (2) correlating findings with clinicopathologic characteristics and data on tumor progression and prognosis.

Design: Tissue microarrays from 164 primary tumors from patients with stage I–III NSCLC were examined. The specimens included 94 adenocarcinomas, 51 squamous cell carcinomas, and 19 large cell carcinomas. Using multiplex immunofluorescence and image analysis, we evaluated PD-L1 expression in malignant cells, $CD68^+$ macrophages, and cells expressing the immune markers CD3, CD8, CD57, CD45RO, FOXP3, PD-1, and CD20. Cell phenotype data were then integrated with clinicopathologic characteristics and next-generation sequencing gene profiles.

Results: PD-L1 expression on malignant cells and other cells was associated with specific clinicopathologic characteristics. In addition, higher densities of antigen-experienced T cells were associated with brain metastases. The most frequent microenvironments in the NSCLC tissues were type II (immunologic ignorance) and type IV (tolerance). Multivariate analysis showed that tumors with (1) brain metastasis; (2) lower densities of T cells, memory T cells, and natural killer T cells; and (3) CD276, CTLA4, MMP-2, and TP53 mutations had worse overall survival compared with tumors without (1) brain metastasis; (2) higher densities of T cells, memory T cells, and natural killer T cells; and (3) tumors without CD276, CTLA4, MMP-2, and TP53 mutations.

Conclusions: We detected different immune cell phenotype and genotype mutations associated with tumor metastases and prognosis in NSCLC. These results should be validated in further studies with larger cohorts.

Practical Application and Validation of the 2018 ATS/ERS/JRS/ALAT and Fleischner Society Guidelines for the Diagnosis of Idiopathic Pulmonary Fibrosis

Lida P. Hariri, MD, PhD[1,3,5*]; Chayanin Nitiwarangkul, MD[2,5,7]; Angela R. Shih, MD[1,5]; Nathaniel Mercaldo, PhD[2,5]; Sarah Mercaldo, PhD[2,5]; Sydney B. Montesi, MD[3,5]; Benjamin W. Roop, BS[3]; Sreyankar Nandy, PhD[3,5]; Ashok Muniappan, MD[4,5]; David A. Lynch, MB, BCh[6]; Amita Sharma, MD.[2,5*]
[1]Department of Pathology, [2]Department of Radiology, [3]Division of Pulmonary and Critical Care Medicine, and [4]Division of Thoracic Surgery, Massachusetts General Hospital, Boston; [5]Harvard Medical School, Boston, Massachusetts; [6]Department of Radiology, National Jewish Health, Denver, Colorado; [7]Department of Diagnostic and Therapeutic Radiology, Ramathibodi Hospital, Mahidol University, Bangkok, Thailand.

Context: Accurate diagnosis of usual interstitial pneumonitis/idiopathic pulmonary fibrosis (UIP/IPF) is essential to inform prognosis and therapeutic decision-making. In 2018, the ATS/ERS/JRS/ALAT and Fleischner Society released new diagnostic guidelines, including the addition of probable UIP as a computed tomography (CT) category. Studies conducted prior to the 2018 guidelines reported that possible/probable UIP has relatively high positive predictive value (PPV) for histopathologic UIP/probable UIP. However, there was variability in PPV and other test characteristics depending on disease prevalence and/or potential sampling bias from use of IPF trial data.

Design: We applied the 2018 ATS/ERS/JRS/ALAT and Fleischner guidelines to a cohort of consecutive patients ($N = 101$) referred for lung biopsy and determined the test characteristics of CTs. The CTs and histopathology were independently evaluated by 2 thoracic radiologists and pathologists, respectively.

Results: Of patients with CT UIP, 84% (95% CI, 63%–94%) had histopathologic UIP with 96% (87%–99%) specificity. Of patients with CT probable UIP, 42% (20%–68%) had histopathologic UIP with 90% (80%–96%) specificity, and 68% (53%–80%) had either histopathologic UIP or probable UIP with 85% (74%–93%) specificity. Patients with CT indeterminate and alternative diagnosis had histopathologic UIP in 23% (11%–42%) and 17% (10%–27%) of cases with specificities of 75% (63%–84%) and 40% (28%–53%), respectively (Table).

Conclusions: We demonstrate that CT UIP and probable UIP has high specificity for histopathologic UIP, and CT UIP has high PPV for histopathologic UIP. In our cohort, CT probable UIP has a PPV of 68% for combined histopathologic UIP/probable UIP. Further studies are needed to assess the PPV of CT probable UIP, including follow-up data to determine patient outcome.

doi: 10.5858/arpa.2020-0650-AB

Test Characteristics of CT Categories for Diagnosis of Histopathologic Usual Interstitial Pneumonitis (UIP)[a]				
	UIP	Probable UIP	Indeterminate for UIP	Alternative Diagnosis
PPV	0.84 (0.63, 0.94)	0.42 (0.20, 0.68)	0.23 (0.11, 0.42)	0.17 (0.10, 0.27)
NPV	0.78 (0.72, 0.83)	0.67 (0.64, 0.71)	0.63 (0.59, 0.68)	0.51 (0.42, 0.59)
Sensitivity	0.47 (0.30, 0.65)	0.15 (0.05, 0.31)	0.15 (0.05, 0.31)	0.24 (0.11, 0.41)
Specificity	0.96 (0.87, 0.99)	0.90 (0.80, 0.96)	0.75 (0.63, 0.84)	0.40 (0.28, 0.53)
κ	0.97 (0.89, 1.00)	0.67 (0.44, 0.85)	0.71 (0.53, 0.85)	0.90 (0.81, 0.96)

Abbreviation: CT, computed tomography.
[a]Test characteristics, including positive predictive value (PPV; eg, Pr[histologic UIP|CT UIP]), negative predictive value (NPV; eg, Pr[not histologic UIP|not CT UIP]), sensitivity (eg, Pr[CT UIP|histologic UIP]), and specificity (eg, Pr[not CT UIP| not histologic UIP]) were determined for all CT categories. The Cohen κ was used to quantify the interrater agreement between the 2 radiologist scores. To quantify the uncertainty of these estimates, 95% CIs or 95% bootstrapped CIs (κ) were computed.

P14/ARF Expression and Immune Microenvironment in Malignant Pleural Mesothelioma

F. Pezzuto[1]; F. Lunardi[1]; F. Fortarezza[1]; S. E. Vuljan[1]; G. Pasello[2]; L. Urso[2]; A. Boscolo[2]; M. Schiavon[1]; F. Rea[1]; F. Calabrese.[1] [1]Department of Cardiac, Thoracic, Vascular Sciences and Public Health, University of Padova, Padova, Italy; [2]Veneto Institute of Oncology (IOV), Padova, Italy.

Context: P14/ARF is an alternate reading frame protein encoded by the *CDKN2A* gene in response to growth stimulation, thus assuming a central role in cell cycle regulation. Its alteration has been reported in many human tumors, and also in malignant pleural mesotheliomas. The association of p14/ARF expression with morphologic features and tumor microenvironment is still unknown.

Design: Diagnostic biopsies from 52 chemonaive pleural mesotheliomas (32 epithelioid, 16 biphasic, and 4 sarcomatoid) were evaluated. Pathologic assessment of necrosis, inflammation, grading, and mitosis was performed. Immunohistochemistry was carried out to evaluate p14/ARF (negative or positive, for nuclear and cytoplasmic staining), PD-L1 (tumor proportion score), and Ki-67 (percentage of positive cells). Different inflammatory cell components ($CD3^+$, $CD4^+$, and $CD8^+$ T lymphocytes; $CD20^+$ B lymphocytes; and $CD68^+$ macrophages) were quantified, distinguishing intratumoral and peritumoral areas (percentage of positive cells). $P14/ARF^+$ patients were compared with $p14/ARF^-$ patients for all demographic and pathologic features.

Results: P14/ARF was detected in 11 patients (21%). $P14/ARF^+$ cases were characterized by higher $CD4^+$ T-lymphocyte percentage (median value, 10% versus 1%; $P = .05$), mainly in peritumoral areas. PD-L1 expression was higher in $p14/ARF^+$ (median value, 50% versus 5%; $P = .05$). No other statistically significant differences were found.

Conclusions: Based on these preliminary data, tumor microenvironment seems to be different in $p14/ARF^+$ mesothelioma patients, thus suggesting a possible influence of the p14/ARF-MDM2-p53 axis. Larger case series are needed to validate these preliminary findings and to improve the statistical power analysis of correlations with clinical data. Experimental studies are ongoing to investigate cellular and functional activities of p14/ARF in mesothelial cells.

Deciphering Molecular Mechanisms of Chemoresistance in Small Cell Lung Cancer (SCLC)

Christiane Kümpers[1]; Mladen Jokic[1]; Carsten Heidel[1]; Anke Fähnrich[3]; Wenzel Vogel[1,2]; Ignacija Vlasic[1]; Finn-Ole Paulsen[1]; Till Olchers[4]; Torsten Goldmann[2,5]; Hanibal Bohnenberger[6]; Philipp Ströbel[6]; Martin Reck[4,5]; Hans Bösmüller[7]; Falko Fend[7]; Jutta Kirfel[1]; Hauke Busch[3]; Sven Perner.[1,2] [1]Institute of Pathology, University Hospital Schleswig-Holstein, Campus Lübeck, Lübeck, Germany; [2]Pathology, Research Center Borstel, Leibniz Lung Center, Borstel, Germany; [3]Institute of Experimental Dermatology, University of Lübeck, Lübeck, Germany; [4]LungenClinic Grosshansdorf, Grosshansdorf, Germany; [5]Airway Research Center North (ARCN), German Center for Lung Research (DZL); [6]Institute of Pathology, University Hospital Göttingen, Göttingen, Germany; [7]Institute of Pathology and Neuropathology University Hospital Tübingen, Tübingen, Germany.

Context: Small cell lung cancer (SCLC) is an aggressive lung cancer with few therapeutic options. This calls for identification of novel targets. We therefore sought to identify the key transcriptomic changes occurring in the chemorelapsed and untreatable SCLC that responded well to first-line chemotherapy. We analyzed the whole transcriptomes of pretherapeutic and posttherapeutic SCLC of the same patient in order to find the key players that might be the focus of targeted therapy for SCLC in the near future.

Design: We identified 26 SCLC patients who responded well to first-line chemotherapy with usable formalin-fixed, paraffin-embedded biopsies of pretreatment tumors and chemorelapsed tumors. After isolating RNA, we performed the Array XS analysis on the tumor tissues covering the whole transcriptome (in total more than 20 000 genes). Findings of the transcriptomic analysis were studied on the protein level by means of immunohistochemistry.

Results: We identified distinct transcriptomic profiles of pretreatment SCLC and their chemorelapsed counterparts, with the most striking difference being the exclusion of immune pathways in the chemorelapsed SCLC. This finding would explain to a certain extent the lack of benefit of immunotherapy in the treatment of SCLC. We also found a number of kinases being upregulated in the chemorelapsed SCLC, indicating that a potential for the targeted treatment of chemorelapsed SCLC exists.

Conclusions: This study gives invaluable insight into the key differences in transcriptomic profiles of chemorelapsed and pretreatment SCLC that could not be analyzed in the past. We believe that the identification of significantly upregulated targetable molecules in chemorelapsed SCLC gives hope for the design of novel targeted therapy.

Diffuse Pulmonary Exogenous Lipoid Pneumonia and Association With Inhalation Exposure to Marijuana or Aerosolized Oil: An Update

P. Pal[1]; Y. Leung[1]; T. AlBaqer[1,2]; Z. Khan[1,3]; R. C. Santiago[1,4]; D. M. Hwang.[1,5] [1]Department of Pathology, University Health Network, Toronto, Ontario, Canada; [2]Departments of Pathology, Sabah Hospital and Kuwait Cancer Control Center, Kuwait City, Kuwait; [3]Department of Pathology, Lakeridge Health System, Oshawa, Ontario, Canada; [4]Department of Pathology, St Luke's Medical Center, Quezon City, Philippines; [5]Department of Laboratory Medicine and Molecular Diagnostics, Sunnybrook Health Sciences Centre, Toronto, Ontario, Canada.

Context: Exogenous lipoid pneumonia results from the ensuing foreign body–type reaction to the presence of exogenous lipid or lipidlike material in the lungs. Here we report a retrospective review of a series of 21 unusual cases of exogenous lipoid pneumonia with diffuse interstitial deposition of exogenous lipoid material.

Design: Cases were identified through review of pathology specimens from patients undergoing lung surgery (volume reduction, lung transplantation, wedge resection, or lobectomy) or cases that were seen for consultation at the Department of Pathology, University Health Network (Toronto, Ontario, Canada), between January 2002 and March 2019.

Results: All 21 cases shared similar histology, consisting of a background of severe emphysema and numerous macrophages predominantly distributed interstitially, containing abundant variably sized, well-delineated intracytoplasmic vacuoles, suggestive of exogenous lipid material. The vacuoles were admixed with varying amounts of brown-black pigment. These macrophages were diffusely distributed throughout the lung tissue, predominantly interstitial, although some were also present within alveolar spaces and showed a predilection for centrilobular distribution. On review of the clinical data, the mean age of these patients was 50 ± 8 years, and a majority of patients were past/present smokers (19 of 21; 90.5%) and had documented exposure to marijuana (9 of 19; 47%). One patient had concurrent adenocarcinoma and 3 had α_1-antitrypsin deficiency. Possible occupational or recrea-

tional aerosolized dust or mineral oil exposure was present in 11 of 21 patients (52%).

Conclusions: Our findings suggest that diffuse exogenous lipoid pneumonia may be associated with inhalational exposure to cannabis and with occupational or recreational exposure to aerosolized oils.

Implementation of a Deep Learning Model at the Clinic by Measuring Tumor Cellularity in Transbronchial Biopsies of Lung Adenocarcinoma

Tomoi Furukawa; Tomoya Oguri; Kishio Kuroda; Yoshiaki Zaizen; Mano Soshi; Junya Fukuoka. Department of Pathology, Nagasaki University Graduate School of Biomedical Sciences, Nagasaki, Japan.

Context: Because of the needs of molecular analysis, pathologists are frequently asked to estimate the percentage of tumor cells in the tissue; however, the process is time-consuming and there is considerable interobserver variability. Our aim was to develop a routine workflow with a deep learning algorithm for measuring tumor cellularity in transbronchial biopsy.

Design: One hundred cases of transbronchial biopsy with lung adenocarcinoma were retrieved from the tissue archive of Nagasaki University Hospital. For the training model, 10 644 annotations from 200 fragments of 40 cases were run in 3 million iterations with HALO AI (Indica Lab, Albuquerque, New Mexico). After the education of the model, segmentation of tumor area by the model was applied for 50 test cases, and the percentage of tumor in each case was calculated using nuclear detection software (Figure 1, A through C). Cases without enough levels of segmentation were excluded. Visual recognition of tumor cellularity by 4 pathologists was obtained independently for the same cases. Numbers from the deep learning model and the pathologists were compared with ground truth (Figure 1, D).

Results: Of 50 testing cases, 29 and 12 showed enough and fair levels, respectively, of segmentation by the educated model. Nine cases were considered poor. Among the 41 cases, average deviations from ground truth were 3% and 4% for the educated model and 16% for pathologists. Deviations for cases with poor segmentation showed an average of 15%.

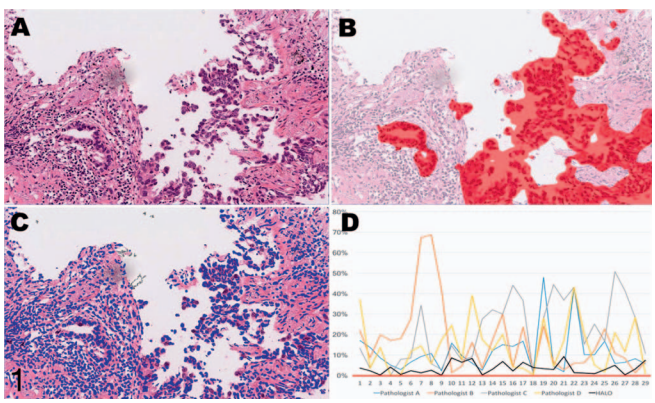

Conclusions: The deep learning model is useful to estimate tumor cellularity in transbronchial biopsy, especially after quality judgement by pathologists.

Feasibility of Cell Block Specimens for Programmed Cell Death Ligand-1 (PD-L1) Immunohistochemistry in Non–Small Cell Lung Cancer (NSCLC)

S. Y. Ha[1]; K. C. Lee[2]; M. G. Pak[3]; M. S. Roh.[3] Departments of [1]Pathology and [2]Radiation Oncology, Gachon University of Medicine and Science, Incheon, Korea; [3]Department of Pathology, Dong-A University College of Medicine, Busan, Korea.

Context: Programmed death ligand-1 (PD-L1) has emerged as a predictive biomarker for immunotherapy in non–small cell lung cancer (NSCLC). In a considerable proportion of NSCLC patients, cytology specimens are often the only specimens available for PD-L1 immunohistochemistry. This study compared the PD-L1 expression between paired cytologic cell block (CB) and surgical specimens and delineated practical feasibility of CB in clinical decision-making for immunotherapy.

Design: Sixty-one eligible patients with primary NSCLC (40 adenocarcinomas, 21 squamous cell carcinomas) who received transthoracic needle aspiration and surgery were included. PD-L1 immunohistochemistry (clone SP263) was performed on CBs and matched surgical resection specimens. Three pathologists individually evaluated the percentage of positive tumor cells, scoring each specimen applying cutoff levels used in clinical studies: <1%, 1%–9%, 10%–49%, and ≥50% positive tumor cells.

Results: A high concordance was found between CB and resection specimens, with Pearson *R* of 0.87. A positive percentage agreement was 94.3%, and a negative percentage agreement was 97.6%, using 1% as the cutoff. The highest agreement (95.1%) between 2 specimens was seen when using ≥50% as cutoff. Disagreement was associated with the tumor being heterogeneous on histology, especially using ≥10% as cutoff. The concordances among 3 pathologists were 0.89 for CB and 0.80 for resection specimens. There was no significant difference according to the time interval that 2 specimens were collected.

Conclusions: These results showed a high concordance between CB and matched resection specimens for PD-L1 immunohistochemistry and suggested that CB specimens could be a valid substrate for the evaluation of PD-L1 expression in NSCLC.

Fine-Needle Aspiration Cytology of Pulmonary Lesions in Granulomatosis With Polyangiitis (GPA, formerly called Wegener's)

W. Elatre; A. Abdelhalim; M. Koss. Department of Pathology, Keck Hospital of University of Southern California, Los Angeles.

A 21-year-old woman was admitted to the hospital with left-sided chest pain, nonproductive cough, shortness of breath, and lower extremity edema/pain. Ultrasound showed bilateral lower and upper extremity deep venous thrombosis. Computerized tomography of the chest revealed bilateral pulmonary opacities and left midlung cavitary lesion. Computed tomography–guided fine-needle aspiration of the lung and bronchial washing/brushing were performed. The cytologic smears showed scattered necrotic tissue fragments entrapping many neutrophils and occasional epithelioid cells. Multinucleated giant cells were occasionally observed. Ziehl-Neelsen stain for acid-fast bacilli was negative. Serum PR3-ANCA was positive. The cytopathologic findings with the clinical manifestations and ANCA value in the serum were consistent with the diagnosis of granulomatosis with polyangiitis (GPA). GPA is a small-vessel vasculitis that leads to focal necrosis within small arteries and veins and is characterized by necrotizing granulomatous inflammation of upper and lower respiratory tracts, glomerulonephritis, and necrotizing vasculitis of the lungs and a variety of systemic organs and tissues. Lung parenchymal disease is the most frequent manifestation, which produces multiple nodules and masses. Early diagnosis and prompt treatment of patients with GPA is essential for a better prognosis. However, the variety of clinical presentations and nonspecific radiologic infiltrates of GPA frequently makes the diagnosis difficult. Sputum cytology, transbronchial biopsy, or fine-needle aspiration cytology is usually needed to confirm diagnosis. GPA may further be distinguished from other small vessel vasculitides by positive serum PR3/c-ANCA.

Lymphoepithelioma-like Carcinoma (LELC): A Case Report of a Rare Tumor of the Lung

W. Elatre; A. Abdelhalim; M. Koss. Department of Pathology, Keck Hospital of University of Southern California, Los Angeles.

The patient, a 59-year-old Asian woman, presented with intermittent chest pain with mild shortness of breath for 2 weeks. Chest x-ray showed a mass lesion in the right lower lung field. Chest computed tomography scan showed a 4-cm, heterogeneously enhanced mass lesion with well-defined margin and lobulated contour in the right middle lobe of the lung, abutting the mediastinum. Bronchoscopy showed no endobronchial lesion. She underwent video-assisted thoracoscopic right lower lobectomy and mediastinal lymph node dissection. An ill-defined nodule with lobular growth pattern containing well-defined solid sheets or small clusters of tumor cells with syncytial pattern separated by broad areas of lymphoplasmacytic reaction, including a few small lymphocytes percolating between carcinoma cells. Tumor cell nuclei were round, oval with mildly irregular nuclear borders, delicate chromatin, and 1 or 2 distinct eosinophilic nucleoli. The pathology, immunohistochemical staining (positive keratin and P63), and positive EBV results confirmed lymphoepithelioma-like carcinoma (LELC) of the lung. Pulmonary LELC is a subtype of large cell carcinoma of the lung according to the

World Health Organization classification. The imaging study findings of primary pulmonary LELC are similar to those of bronchogenic carcinomas in the majority of cases. LELC of the lung may be mistaken histopathologically for metastatic nasopharyngeal carcinoma or lymphoma, resulting in improper patient management. LELC should be considered in the differential diagnosis of primary lung tumors, particularly when an extensive lymphocytic infiltrate is observed. Clinicians, pathologists, and radiologists may encounter primary pulmonary LELC on imaging or at biopsy procedure; consequently, familiarity with this distinct entity is required.

Computed Tomography Radiomics to Assess Pathologic Grade of Lung Adenocarcinomas

J. R. Ferreira-Junior[1]; S. S. Batah[2]; J. R. Machado-Rugolo[2]; A. T. Fabro[2]; M. Koenigkam-Santos[1]; P. M. Azevedo-Marques.[1] [1]Center of Imaging Sciences and Medical Physics and [2]Department of Pathology and Legal Medicine, Ribeirão Preto Medical School, University of São Paulo, Brazil.

Context: To perform a radiomics analysis by associating quantitative features from computed tomography images with pathologic grades of lung adenocarcinomas.

Design: One hundred one patients with lung cancer diagnosed and treated at our hospitals from 2010 to 2017 with definitive surgical/pathologic diagnosis were used. Tumor grading was based on the 2011 International Association for the Study of Lung Cancer/American Thoracic Society/European Respiratory Society (IASLC/ATS/ERS) classification: grade 1 (lepidic), grade 2 (acinar or papillary), and grade 3 (solid or micropapillary). Pretreatment contrast-enhanced computed tomography images were semiautomatically segmented using volumetric region growing algorithm (3D-Slicer v4.3.1, Boston, Massachusetts). Tumors were characterized by 2465 radiomic features extracted from segmented images (Ibex v1.0, Houston, Texas), such as gray-level intensity (number of features: 53), histogram (51), co-occurrence matrix (550 in 2D and 1540 in 3D), run-length matrix (33) and shape (18).

Results: Of the 101 patients, 58 had adenocarcinoma, from which 7 were grade 1, 15 were grade 2 (10 acinar, 5 papillary), and 6 were grade 3 (all solid). Two radiomic features were significantly associated with tumor grading: correlation and information measure of correlation, both obtained from the gray-level co-occurrence matrix. Additionally, other features were statistically associated when comparing pairs of groups, for instance skewness from a Laplacian of Gaussian filter (grade 1 versus grade 2), fractal dimension estimation (grade 1 versus grade 3), and mean breadth from shape (grade 2 versus grade 3).

Conclusions: Gray-level co-occurrence matrix, which measures linear dependencies of intensity values of an image, presented great potential as a computed tomography radiomic feature to noninvasively assess pathologic grade of lung adenocarcinomas at a macroscopic level.

Clinical Impact of Paracoccidioidomycosis-Induced Pulmonary Hypertension

A. T. Fabro[1]; S. S. Batah[1]; P. S. Leão[1]; M. A. Alda[1]; R. G. Felix[1]; J. Machado-Rugolo[2]; V. L. Capelozzi[2]; R. Duarte Achcar.[3] [1]Pathology and Legal Medicine, Medical School of Ribeirao Preto, University of São Paulo, Brazil; [2]Pathology, Faculty of Medicine, University of São Paulo, Brazil; [3]Department of Medicine, Pathology Division, National Jewish Health, Denver, Colorado.

Context: Although effective treatment is available to control paracoccidioidomycosis (PCM) infection, many patients considered clinically cured develop pulmonary hypertension as a late sequel. We investigated the clinical impact of pulmonary hypertension in human pulmonary PCM subjects.

Design: A total of 510 patients diagnosed with PCM were evaluated during a 10-year period (2007–2017). Hematoxylin-eosin, picrosirius red stain, and morphometry were performed.

Results: Most of the patients were men between 50 and 60 years old and chronic smokers. One-third of the patients had chronic obstructive pulmonary disease and a mean of 67-pack-year smoking history. Of 510 patients, only 16 (3.14%) had echocardiography performed and none of those had right cardiac catheterization. Fifty percent of these patients (n = 8) had an aggressive phenotype with progressive pulmonary hypertension with pulmonary artery systolic pressure >35 mm Hg and increased right ventricular systolic pressure, after clinical cure of PCM, whereas the other 50% (n = 8) had a stable phenotype (pulmonary artery systolic pressure ≤35 mm Hg). No clinical, radiologic, or pathologic parameters differentiated these 2 phenotypes of pulmonary hypertension, including smoking pack-year history or chronic obstructive pulmonary disease. Vascular remodeling by adventitial changes was demonstrated in lung surgical biopsy.

Conclusions: To the best of our knowledge, this is the first study to report this PCM-associated late complication. Aggressive outcome with progressive pulmonary hypertension levels occurs in late-stage post–PCM clinical cure, and we recommend screening echocardiogram and long-term clinical follow-up for pulmonary hypertension in all patients with PCM.

Immune Checkpoint Gene Polymorphism and Immunoprofiling Data Improve Prediction of Risk of Brain Metastases and Death in Lung Cancer

J. Machado-Rugolo[1]; S. S. Batah[2]; A. T. Fabro[2]; V. L. Capelozzi.[3] [1]Clinics Hospital, Botucatu Medical School, São Paulo State University (UNESP), Botucatu, São Paulo State, Brazil; [2]Department of Pathology, Ribeirão Preto Medical School, University of São Paulo (USP), Ribeirão Preto, Brazil; [3]Department of Pathology, São Paulo Medical School, University of São Paulo (USP), São Paulo, Brazil.

Context: Immune checkpoint blockade has emerged as a novel therapy against cancer and has been suggested to improve survival of non–small cell lung carcinoma patients. This study investigated whether polymorphisms of immune checkpoint genes are associated with the tumor immune cell profile and with brain metastasis risk and death of patients with advanced non–small cell lung cancer.

Design: Seventy-five advanced non–small cell lung cancer patients were studied. Expression of PD-L1, CD68, CD3, CD8, CD57, CD45RO, FOXP3, PD-1, and CD20 was evaluated by multiplex immunofluorescence and image analysis using a VectraMTPolaris multispectral microscope (Akoya Biosciences Inc, Hopkinton, Massachusetts). Single-nucleotide variants in *PD-L1*, *CTLA-4*, *PD-L2*, *LAG3*, and *B7H4* genes were evaluated with high-throughput sequencing by TruSeq Custom Amplicon Panel (Illumina). Expression and gene profile data were integrated with clinicopathologic characteristics for different models to predict death risk using Cox regression analysis.

Results: A significant association was found between CTLA-4 (AG genotype) and $CD20^+$ lymphocytes ($R = -0.32$, $P = .02$). Low risks of brain metastasis and death for patients in N1 stage (β coefficient = 3.24, $P = .01$) and CTLA-4-rs231775-AG genotype (β coefficient = −3.71, $P = .04$) were observed. The risk of death was related to CD274-rs2297136-GA genotype (β coefficient = −8.55, $P = .03$), LAG3-rs870849-TC genotype (β coefficient = 2.16, $P = .04$), low density of PD-L1 (β coefficient = 6.43, $P = .04$) and high density of $CD3^+CD8^+$ lymphocytes (β coefficient = −3.06, $P = .04$).

Conclusions: Incorporating immune checkpoint gene polymorphisms into immunoprofiling score improves prediction of brain metastases and death in advanced non–small cell lung cancer. Our results suggest immune-based therapies may play a leading role, depending on the immune checkpoint gene polymorphism profile.

Primary Adenoid Cystic Carcinoma of the Lung With High-Grade Transformation

N. Iranzad; J. Carney. Department of Pathology, Duke University Medical Center, Durham, North Carolina.

Adenoid cystic carcinoma of the lung is a rare entity. Although high-grade transformation of adenoid cystic carcinoma of the head and neck has been recognized, this phenomenon has not been previously reported in the lung. Herein, we present a case of a 72-year-old man with a 55-pack-year smoking history who presented with an incidental finding on chest imaging of a solitary right upper lobe mass. The patient's history was otherwise significant for squamous cell carcinoma of the mandible, for which he underwent resection and adjuvant radiation therapy. A positron emission tomography scan confirmed a right upper lobe hypermetabolic mass concerning for primary lung cancer with no evidence of nodal or metastatic disease. A needle core biopsy of the lung mass demonstrated carcinoma with basaloid features, necrosis, and stroma compatible with adenoid cystic carcinoma. The patient subsequently underwent a right upper lobectomy. Microscopic examination of the tumor showed features typical of adenoid cystic carcinoma, including cribriform and trabecular growth patterns and minimal necrosis. However, other sections sampled demonstrated a solid growth pattern with comedo-type necrosis as well as high-grade cytologic features and loss of myoepithelial differentiation, changes compatible with high-grade transformation. Immunohistochemistry was performed and the tumor staining profile is shown in the Table. High-grade transformation of adenoid cystic

carcinoma is uncommon, and its occurrence in the lung has not been previously reported. Recognition of this unusual variant is an important diagnostic consideration on small biopsies and resection specimens for suspected primary pulmonary malignancies.

Immunohistochemistry Profile	
Positive	**Negative**
Pan-cytokeratin	TTF-1
SOX10	CD117
p40 (patchy)	Calponin
CD56 (patchy)	Smooth muscle actin
	Synaptophysin
	S100
	CD1a

Histopathologic Changes Induced by Pleural Sealants Used During Transthoracic Needle Core Biopsy (TTNB) and Their Impact on Lung Cancer Resection Specimen Staging

A. Bodolan; B. Bryant; A. Schned; K. Butnor. Department of Pathology and Laboratory Medicine, University of Vermont Medical Center, Burlington.

Context: Patients undergoing transthoracic needle core biopsy (TTNB) of the lung are at risk for biopsy-related pneumothorax. Instilling pleural sealant at the pleural puncture site reduces this risk.

Design: The histologic changes associated with pleural sealant and their impact on assessing pathologic stage in lung cancer resection specimens have not been previously evaluated. The pathologic findings in all lung cancer resection specimens in which pleural sealant was used during TTNB in 2015–2018 were retrospectively reviewed.

Results: Thirty-three cases were identified. TTNB preceded lobectomy by an average of 35 days. Amphophilic crinkled pleural sealant material (Figure 2) was associated with tumors in 14 cases (42%), including 10 adenocarcinomas, 2 squamous cell carcinomas, and 2 pleomorphic carcinomas, which averaged 1.7 cm in greatest dimension. Surrounding the sealant material was a 0.2–1.0 cm in greatest dimension pseudocystic space lined by histiocytes and multinucleated giant cells that occupied, on average, 14% of the tumoral area. Although pleural sealant did not adversely impact assessment of pathologic stage in any of the cases, it potentially could have in 1 case by obscuring the visceral pleural elastic layer, but definitive visceral pleural invasion was present in an adjacent section.

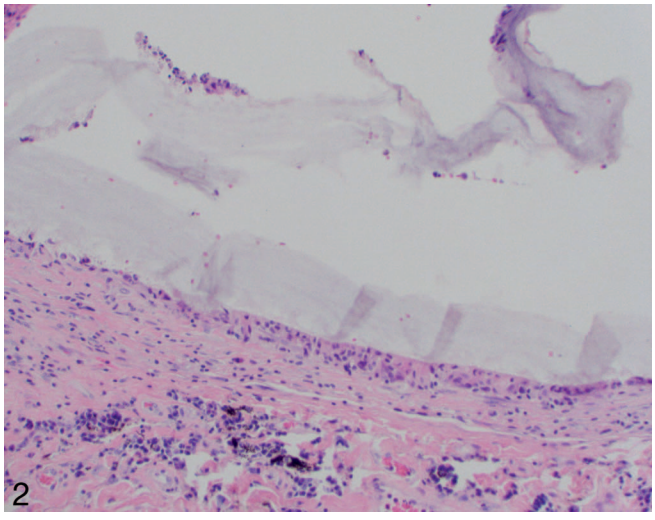

Conclusions: Pleural sealant instilled during TTNB has the potential to obscure histologic features that are important for accurate staging of subsequent lung cancer resection specimens. In practice, pleural sealants appear to have little or no adverse impact on assessment of pathologic stage in lung cancer resection specimens. Recognizing the histologic appearance of pleural sealant and its associated tissue response is important to avoid diagnostic misinterpretation.

Kaposiform Lymphangiomatosis: An Unusual Case Occurring in an Adult Male

X. Cheng[1]; Q. Tan[2]; A. Takano.[1] Departments of [1]Anatomical Pathology and [2]Respiratory & Critical Care Medicine, Singapore General Hospital, Singapore.

Kaposiform lymphangiomatosis is a rare variant of lymphangiomatosis usually encountered in pediatric patients. This is the third case reported in an adult at time of writing, with added twists being the presence of coexisting lung adenocarcinoma as well as the spindle cell proliferation seen first on transbronchial biopsy, which was challenging to characterize in a limited sampling of this unusual entity. A 48-year-old Chinese man presented with chronic cough, dyspnea, and fever of 4 months' duration. He had left-sided infiltrates on chest x-ray, persisting despite oral antibiotics. Sputum tuberculosis tests were negative. A computed tomography scan revealed extensive infiltrating soft tissue in the mediastinum and left tracheobronchial tree, a small pericardial effusion, and a right upper lobe 1.9-cm consolidative focus. All of these areas were hypermetabolic on positron emission tomography. At that time, clinical suspicion was high for malignancy. Bronchoscopy showed diffuse infiltration of the tracheobronchial tree from trachea to carina and left and right main bronchi. Transbronchial lingular biopsies yielded a peribronchial bland spindle cell proliferation, positive for CD31. Resampling was recommended, and wedge resection showed thickened septa containing dilated D2-40–positive lymphatic channels with admixed nodular spindle cell (kaposiform) proliferations; the latter were $CD31^+$, factor $VIII^+$, and $HHV\text{-}8^-$, with 1% Ki-67 index. Findings were in keeping with kaposiform lymphangiomatosis. Biopsy of the right upper lobe nodule with subsequent right upper lobectomy revealed lepidic-predominant adenocarcinoma, positive for epidermal growth factor receptor exon 20 duplication on molecular analysis. Currently, the patient is being monitored postoperatively for consideration of sirolimus treatment for lymphangiomatosis.

Resected Pulmonary Mass Lesions in Pediatric Patients: A Clinicopathologic Study of 368 Cases

S. Terra; S. M. Knight; B. R. Kipp; J. M. Boland. Department of Laboratory Medicine and Pathology, Mayo Clinic, Rochester, Minnesota.

Context: Resected mass lesions in children demonstrate a different disease profile than those in adults, which can lead to diagnostic difficulties for pathologists. Special attention must be given to nonneoplastic conditions (congenital abnormalities, infectious disease). Primary lung neoplasms in children are rare, and metastases often represent rare tumors (sarcomas). We sought to better characterize the spectrum of disease in resected mass lesions from pediatric patients.

Design: Institutional pathology archives were searched from 1992 to 2017 for patients $\leq$21 years with surgically resected lung mass lesions. Slides and clinical information were reviewed.

Results: Lung mass lesions were resected in 368 pediatric patients. Primary neoplasms occurred in 23 (6%; mean age, 13.7 years; range, 6 months–21 years), most often carcinoid tumor (10; 2 atypical), inflammatory myofibroblastic tumor (4), adenocarcinoma (2; both in the setting of prior malignancy), and pleuropulmonary blastoma (2). Metastatic disease was observed in 187 (51%; mean age, 14.4 years; range, 1–21 years), most commonly osteosarcoma (71; 40% of metastases), germ cell tumor (24), Ewing sarcoma (20), Wilms tumor (17), rhabdomyosarcoma (9), and classical Hodgkin lymphoma (9). Cysts and malformations were resected in 58 patients (16%), including congenital pulmonary airway malformations (32) and sequestrations (12). The remaining 100 patients (27%) had various nonneoplastic diagnoses: necrotizing granuloma (33), intrapulmonary lymph node (16), abscess/infection (14), and organizing pneumonia (11).

Conclusions: In children, metastases and infectious/inflammatory lesions are the most common resected mass lesions. Primary lung neoplasms constitute a small minority and are most commonly carcinoid tumors. Lung adenocarcinomas rarely occur in children, especially in the setting of prior malignancy.

Liposarcoma of the Pleural Cavity

T. Kawai[1]; T. Yokose[2]; K. Washimi[2]; T. Matsuo.[3] [1]Toda Central Medical Laboratory/National Defense Medical College, Toda/Tokorozawa, Japan; [2]Department of Pathology, Kanagawa Cancer Center, Yokohama, Japan; [3]Department of Surgery, Saiseikai Omuta Hospital, Omuta, Fukuoka, Japan.

Context: Liposarcoma rarely occurs in the pleura or thoracic cavity, and few cases appear in the literature. We hypothesized that combining clinicopathologic, immunohistochemical, and fluorescence in situ hybridization methods would allow definite diagnoses.

Design: Using formalin-fixed, paraffin-embedded blocks, we examined 1 atypical lipomatous neoplasm/well-differentiated type (case 3) and 2 dedifferentiated liposarcomas (cases 1 and 2).

Results: Mean age was 52 years (range, 43–62 years) in 2 men and 1 woman. Each case exhibited a well-circumscribed mass. Histologically, case 1 exhibited round to oval tumor cells with a high nucleus to cytoplasm ratio that had proliferated in nests, accompanied by some giant cells but no fatty cells. Case 2 displayed 2 components: a lipogenic area and atypical spindles of mildly pleomorphic cells arranged in a storiform pattern. Case 3 exhibited a well-differentiated liposarcoma with some lipoblasts. Immunohistochemically, all cases were positive for both S-100 and p16. Case 3 was positive for adipophilin, but negative for CDK4 and MDM2. Cases 1 and 2 were positive for CDK4 and MDM2, but only case 1 was positive for both CD99 and adipophilin. Case 1 exhibited *MDM2* amplification by fluorescence in situ hybridization (Vysis LSI MDM2 SpectrumOrange Probe plus Vysis CEP 12 SpectrumGreen Probe, Abbott Molecular, Abbott Park, Illinois). All patients are alive after 6.5 years (case 1), 5 years (case 2), and 1 year (case 3).

Conclusions: For a firm diagnosis of liposarcoma in the pleura, immunohistochemistry for CDK4, MDM2, and adipophilin together with *MDM2* gene amplification by fluorescence in situ hybridization may be an important diagnostic tool.

Mucinous Adenocarcinomas of the Lung Presents Particular Subtypes

Carlos Faria[1]; Vânia Almeida[1,2]; João Fraga[1]; Vítor Sousa[1,2,3,4]; Lina Carvalho.[1,2,3,4] [1]University Hospital Anatomical Pathology, Coimbra, Portugal; [2]Institute of Anatomical and Molecular Pathology, [3]CIMAGO Research Center for Environment, Genetics and Oncobiology, and [4]Centre of Pulmonology, Faculty of Medicine, University of Coimbra, Coimbra, Portugal.

Context: World Health Organization (WHO) classification (2015) of the mucinous adenocarcinomas of the lung includes invasive mucinous adenocarcinoma and mixed invasive mucinous/nonmucinous. The previous 2004 WHO classification classified mucinous adenocarcinomas as a subtype of bronchioloalveolar carcinoma. Different patterns of primitive mucinous adenocarcinomas may provide prognostic information.

Design: Surgically resected mucinous adenocarcinomas of the lung were selected for comprehensive morphologic comparison and immunohistochemical assessment.

Results: "Pure" patterns of primitive mucinous adenocarcinomas of the lung may be recognized by use of immunohistochemistry, as shown in the Table. After exclusion of a young female patient with multifocal mucinous adenocarcinoma in situ, colloid mucinous adenocarcinoma, and cystic adenomatoid malformation related to mucinous adenocarcinomas from the study cohort, 6 independent subtypes of pulmonary adenocarcinomas were identified.

Conclusions: Specific immunophenotypes in primary mucinous adenocarcinomas of the lung may reflect carcinogenesis and may represent a foundation for potential molecular targeted therapies.

Summing Up of the Pure Patterns[a]

	Age	Sex	PAS	TTF1	CK7	CK20	CDX-2	VIM
Mucinous acinar adenocarcinoma	78	M	+++	−	+++	−	−	−
Mucinous acinar/papillary adenocarcinoma of enteric type	70	F	+++	++	+++	++	++	−
Solid mucinous adenocarcinoma	63	M	+++	−	+++	−	−	−
Solid mucinous adenocarcinoma of enteric type	62	M	+++	−	+++	−	−	−
Mucinous micropapillary adenocarcinoma	70	F	+++	+++	+++	−	−	+
Mucinous cell adenocarcinoma	74	F	+++	−	+++	−	−	+

[a]CD56, CK5.6, and p63 had no expression.

Mucinous Adenocarcinoma in Congenital Pulmonary Airway Malformation

Vânia Almeida[1,4]; Ana Alarcão[1,2,3]; Ana Filipa Ladeirinha[1,2]; Maria Reis Silva[1,2,3]; Teresa Ferreira[1,2]; Ana Isabel Rodrigues[1]; Vitor Sousa[1,2,3,4]; Lina Carvalho.[1,2,3,4] [1]Institute of Anatomical and Molecular Pathology, Faculty of Medicine, University of Coimbra, Portugal; [2]CIMAGO Research Center for Environment, Genetics and Oncobiology, Faculty of Medicine, University of Coimbra, Coimbra, Portugal; [3]Centre of Pulmonology, Faculty of Medicine, University of Coimbra, Portugal; [4]Anatomical Pathology, University Hospital, Coimbra, Portugal.

Congenital pulmonary airway malformation (CPAM) is a rare developmental malformation of the lower respiratory tract and is recognized as a preinvasive lesion for mucinous adenocarcinoma (IMA). We present a case of CPAM associated with IMA detected in a 76-year-old woman. A computed tomography scan was performed because of chronic pancreatitis, showing a lung lesion suspicious of lung cancer. Positron emission tomography revealed a 4.7 × 4.2-cm functionally heterogeneous and multicystic mass. Bronchial brushing/aspirate was negative for neoplastic cells; transthoracic needle biopsy diagnosed an adenocarcinoma. A left lower lobectomy was performed. On gross examination, a 6 × 5.5 × 4.5-cm white/gelatinous mass eroding the pleura was detected. Histologic analysis showed mucinous bronchioloalveolar pattern with goblet cells and basally located nuclei intermingled with mucinous acinar pattern. Tumoral cells expressed CK7/TTF-1, focal CK20, and no CDX2. Adjacent/2 cm around the tumor, a CPAM Stokes type I lesion with foci of goblet cell hyperplasia was identified. Eighteen hilum/mediastinum lymph nodes had no metastatic disease. IMA in the context of CPAM Stokes type 1 was reported. Both CPAM and IMA lesions were found to be microsatellite stable. Immunohistochemistry for mismatch repair proteins was positive in both CPAM and IMA. *KRAS* somatic mutation c.35G>A;p.(Gly12Asp) detected on IMA was absent on CPAM. This case illustrates the possible diagnosis of CPAM in older patients and highlights the need to explore the relationship of *KRAS* and microsatellite instability in IMA carcinogenesis developed from CPAM lesions.

MDM2 as a Predictor of Hyperprogression in Lung Cancer Patients Treated With Immunotherapy

E. Moreno[1]; A. Barquin[2]; M. E. Reguero[1]; A. Santon[1]; M. E. Olmedo[2]; A. Benito.[1] Departments of [1]Pathology and [2]Medical Oncology, Hospital Universitario Ramón y Cajal, Madrid, Spain.

Context: Immunotherapy has become a standard of care in lung cancer patients. Hyperprogression (paradox response with dramatic tumor surge and clinical worsening) has been recently reported. Predictors of hyperprogression have not been clearly defined. Clinical factors like age, prior radiotherapy, or metastatic burden have been proposed. *MDM2* amplification or EGFR alterations are possible biomarkers of poor outcome.

Design: We reviewed a series of 9 lung cancer patients treated with immunotherapy fulfilling hyperprogression criteria. We performed fluorescence in situ hybridization study of *MDM2* in all cases and summarize the molecular profile, histologic findings (including PD-L1 status) and therapy received.

Results: The most common histology was adenocarcinoma (6) followed by squamous cell carcinoma. Mean patient age was 65 years (54–72 years) and 7 patients had 2 or more metastatic sites. Three patients had *KRAS* mutations. We detected *MDM2* amplification in one patient treated with anti-PD-1/PD-L1 monotherapy. Other cases in the study had gene amplification not reaching the cutoff point used.

Conclusions: Proposed biomarkers associated with hyperprogression are age >65, >2 metastatic sites, and radiotherapy before starting treatment. Six patients in our series were age >65, 3 had received radiotherapy, and 7 had >2 metastatic sites when they received immunotherapy. *MDM2* amplification rate in stage IV lung patients is low (<5%) but more than 65% of them suffer hyperprogression. *MDM2* was amplified in 11% of patients in our series selected by clinical hyperprogression, but could be higher if less strict criteria were used. Although larger studies are needed, molecular profiling of patients including MDM2 could be useful to select patients for immunotherapy.

Industrial Silicone–Induced Acute Lung Injury

E. Ely[1,2,3]; K. Sabharwal[3]; M. Graham.[1,2,3] [1]Department of Pathology, St Louis University School of Medicine, St Louis, Missouri; [2]City of St Louis Medical Examiner's Office, St Louis, Missouri; [3]St Louis County Medical Examiner's Office, St Louis, Missouri.

Context: The popularity of buttock augmentation has been increasing. Food and Drug Administration (FDA)–authorized procedures for buttock augmentation include fat transfer and insertion of silicone implants. A less expensive alternative procedure, albeit not FDA approved, involves injecting liquid silicone into the buttocks. These illicit procedures typically involve administration of industrial silicone by nonmedical personnel in nonmedical facilities. Injection of liquid silicone, often in large quantities, occasionally causes adverse effects, one of which is pulmonary embolization leading to acute lung injury.

Design: We report 2 cases of fatal acute lung injury consequent to silicone embolization complicating liquid silicone buttock injections.

Results: Two previously healthy adult women underwent buttock silicone injections administered by nonmedical personnel in nonmedical settings. Shortly after undergoing the procedures, each woman complained of not feeling well. Each developed progressive respiratory distress and was taken to the hospital. Each patient was hypoxic and developed features of acute respiratory distress syndrome. Their hospital courses were characterized by acute respiratory distress syndrome with superimposed multisystem organ failure. Their deaths occurred 4 and 6 days after the injection procedures. At autopsy, there was extensive acute lung injury. The pulmonary microvasculature contained extensive silicone droplets. Silicone was also present in the buttocks. Octamethylsiloxane and heptamethylsiloxane were identified in the blood of one of the decedents.

Conclusions: Clandestine injection of liquid silicone can lead to acute lung injury. Establishing the cause of acute lung injury may involve obtaining an accurate history, lung biopsy, identification of injected sites/material, autopsy, and specialized laboratory analyses. Correctly establishing and documenting the diagnosis has significant public health and legal ramifications.

How Reliable Is the Ki-67 Proliferative Index in the Assessment of Metastatic Neuroendocrine Tumors?

H. Shirsat; A. Basu; N. Narula; A. Simms; A. Moreira; F. Zhou. Department of Pathology, NYU School of Medicine, New York, New York.

Context: In the diagnosis of metastatic neuroendocrine tumors, crush artifact may preclude mitotic counting, in which case Ki-67 proliferative index (KPI) becomes important for grading of well-differentiated neuroendocrine tumors (WDNETs). Few studies have examined reliability of KPI in the grading of metastatic WDNETs.

Design: Retrospective pathology database review (2008–present) identified 16 patients with metastatic WDNET: 1 thymic, 5 lung, 9 enteropancreatic, and 1 middle ear adenoma. Four of 16 patients had multiple metastases, for a total of 22 metastases. KPIs were compared between primary and metastasis.

Results: Among the lung atypical carcinoids (ACs), 3 metastases had higher KPIs than primaries (50% versus 40%, 15% versus 5%, 30% versus 15%), 2 had lower KPIs (5%–7% versus 25%–30%), and 1 had the same KPI (25%). In the thymic AC (KPI 20%), a supraclavicular node metastasis showed extensive crush artifact and high KPI (70%), raising the possibility of small cell carcinoma. Pericardial metastasis had KPI 40%. In the middle ear adenoma (KPI 5%), KPIs in metastases were 15%–30%. In the 10 metastases from 9 enteropancreatic neuroendocrine tumors, 3 had higher KPI (5%), which classified them as grade 2, whereas primary was grade 1 (KPI 1%). Seven had similar KPI/grade to primary, and none had lower KPI (Table).

Conclusions: Several cases of metastatic WDNET displayed higher or lower KPIs representing potential diagnostic pitfalls, especially when significant crush artifact precludes morphologic evaluation or in cases of metachronous metastases. In metastatic WDNETs, grading using KPI must be done cautiously with a caveat that overgrading or undergrading may occur. The significance of higher KPIs in metastases is unknown and needs further evaluation.

Table of Primary WDNET and Metastasis With Their Respective Ki-67 Proliferative Indices

Primary Diagnosis	Site	KPI, %	Metastatic Site	KPI, %
Atypical carcinoid	Lung	25	Hilar LN	25
Atypical carcinoid	Lung	25	Hilar LN	5
Atypical carcinoid	Lung	30	Liver	7
Atypical carcinoid	Lung	15	Adrenal gland	30
Atypical carcinoid	Lung	5	Liver	15
Atypical carcinoid	Lung	40	Mediastinal LN	50
Atypical carcinoid	Thymus	20	Pericardium	40
Atypical carcinoid	Thymus	20	Supraclavicular LN	70
Middle ear adenoma	Middle ear	5	Lateral neck LN, upper	30
Middle ear adenoma	Middle ear	5	Lateral neck LN, lower	20
Middle ear adenoma	Middle ear	5	Brain	25
Middle ear adenoma	Middle ear	5	Preauricular mass	15
WDNET grade 1	Small bowel	<1	Mesenteric LN	<1
WDNET grade 1	Small bowel	<2	Small bowel recurrence	<2
WDNET grade 1	Small bowel	<2	Liver	5
WDNET grade 1	Small bowel	1	Mesenteric nodule	5
WDNET grade 1	Small bowel	1	Liver	5
WDNET grade 1	Small bowel	1	Liver	5
WDNET grade 2	Small bowel	10	Liver	20
WDNET grade 1	Colon	<5	Peritoneal implants	2
WDNET grade 1	Colon	<5	Ovary	5
WDNET grade 3	Pancreas	30	Liver	30

Abbreviations: KPI, Ki-67 proliferative index; LN, lymph node; WDNET, well-differentiated neuroendocrine tumor.

Pulmonary Ciliated Muconodular Papillary Tumor (CMPT) With Nonclassic Morphology: Potential Pitfall in Frozen Section and Small Biopsy Diagnosis

H. Shirsat; F. Zhou; A. Basu; A. Simms; A. Moreira; N. Narula. Department of Pathology, NYU School of Medicine, New York, New York.

Context: Pulmonary ciliated muconodular papillary tumors (CMPTs) are rare benign peripheral lung tumors with classic and nonclassic subtypes. Radiologically, on frozen sections, and biopsies, these can be misdiagnosed as malignancy.

Design: We describe the radiologic and pathologic features of 1 classic CMPT and 2 nonclassic CMPTs and discuss the potential pitfalls in small biopsies and frozen sections.

Results: The classic CMPT was a solid nodule on CT scan with a standardized uptake value (SUV) of 5.4. A diagnosis of CMPT was favored on the frozen section that showed glandular and papillary patterns lined by ciliated, goblet, and mucin-producing cells and subsequently confirmed by immunohistochemical staining with TTF-1 and p40. Immunostain for BRAF V600E was focally positive. One of the nonclassic CMPTs was a solid and ground glass spiculated nodule with an SUV of 1.4. A biopsy showed few mildly atypical cells that were p40 positive and diagnosed as suspicious for squamous cell carcinoma. The frozen section was called non–small cell lung carcinoma. The permanent sections showed lepidic and acinar patterns lined by a bilayer consisting of TTF-1– and p40-positive cells. Immunostain for BRAF V600E was negative. The second patient with nonclassic CMPT had nonspecific findings on CT scan with nodules. This patient underwent wedge resection that showed a nodule with glandular pattern lined by ciliated cells and p40-positive basal cells.

Conclusions: Careful evaluation of the epithelial lining cells that consist of a mixture of ciliated columnar, goblet, and mucin-producing cells in biopsies and frozen sections may prevent misdiagnosis of CMPT as malignancy.

Lung Adenocarcinomas With Multifocal Nodules May Have a Low Rate of Recurrence Irrespective of Morphologic or Molecular Stages

D. Suster; Z. Ordulu; D. Dias-Santagata; M. Kem; J. Iafrate; M. Mino-Kenudson. Department of Pathology, Massachusetts General Hospital, Harvard Medical School, Boston, Massachusetts.

Context: Distinguishing multiple synchronous primaries (SPs) from intrapulmonary metastasis in lung adenocarcinoma can be difficult. Molecular profiling may help provide more accurate T staging for cases with multiple nodules.

Design: Patients with 2 or more adenocarcinomas resected at a single operation from 2002 to 2016 were selected. Multiplex polymerase chain reaction assay and/or next generation sequencing (NGS) were performed on multiple tumor nodules. Tumors were compared and staged based on histomorphologic patterns and characteristics. They were also staged according to molecular results. Outcomes were correlated with tumor staging.

Results: The study consisted of 3 groups: (1) multiple lepidic predominant lesions (n = 4); (2) lepidic-predominant and non–lepidic-predominant adenocarcinomas (n = 10); and (3) multiple invasive adenocarcinomas (n = 21). In groups 1 and 2, genetic profiles were different among multiple lesions in all except 1 case (group 2). In group 3, histology classified 18 cases as SP and 3 as intrapulmonary metastasis; molecular profiling classified 16 cases as SP and 5 as intrapulmonary metastasis. The overall discordance between histologic and molecular staging for group 3 was 24% (5 of 21 cases). Molecular profiling upstaged 3 cases and downstaged 2 cases. Of the 19 patients in group 3 with available follow-up (mean, 4.7 years), only 1 (SP by both assessments) experienced recurrence, whereas 4 patients (SP by both assessments) developed a new adenocarcinoma.

Conclusions: The results indicate that many lepidic-predominant lesions are independent tumors. In addition, although a significant fraction of cases with multiple invasive adenocarcinomas have discrepant histologic and molecular T stages, it appears that regardless of the differences the rate of recurrence is low.

NUT Carcinoma of the Lung: An Underdiagnosed Entity?

T. Losmanová; C. Neppl; S. Berezowska. Institute of Pathology, University of Bern, Bern, Switzerland.

Context: Primary pulmonary NUT carcinoma was introduced with the 2015 World Health Organization classification of lung tumors as a rare, aggressive, poorly differentiated carcinoma with characteristic foci of keratinization and defining *NUT* rearrangement. After diagnosing our first case in a 45-year-old woman with lung cancer metastasized to the brain, we aimed to determine the frequency of NUT tumors in our cases of lung cancers with squamous morphology or brain metastases.

Design: NUT was retrospectively analyzed by immunohistochemistry in our single-center cohorts of 403 consecutive tumors diagnosed as primary pulmonary squamous cell carcinoma, resected from 2000 to 2013, and 192 consecutive brain metastases from lung cancer primaries, resected from 2000 to 2016. Staining was conducted on tissue microarrays.

Results: Staining could be evaluated in 384 of 403 and 173 of 192 tumors, respectively, because of technical reasons. Finally, 555 patients were analyzed, 404 with squamous morphology, 22 of those including brain metastases. One hundred fifty-one brain metastases originated from nonsquamous lung cancers. The median age was 69 years (range, 43–85 years) for the primary squamous cell carcinoma cohort and was 61 years (range, 30–82 years) for the brain metastases cohort, with 11 and 23 patients, respectively, being younger than 50 years. Forty-five percent of primary squamous cell carcinomas were poorly differentiated (G3). None of the tumors expressed NUT.

Conclusions: Our results emphasize NUT carcinoma as a very rare entity in the lung. Despite these findings, NUT carcinoma must be considered in the differential diagnosis of undifferentiated tumors with focal squamous differentiation, especially for the potential future use of molecular target therapy in these tumors.

What Are the Growth Patterns of the Advancing Edge of Squamous Cell Carcinomas of the Lung?

S. Shyu; R. E. Fanaroff; A. P. Burke. Department of Pathology, University of Maryland Medical Center, Baltimore.

Context: The growth patterns at the periphery of squamous carcinomas of the lung are variable, and little is known about alveolar spread.

Design: One hundred three tumors were retrospectively reviewed. Advancing features were classified as intra-alveolar (tumor growth within intact alveolar spaces without reactive pneumocytes); tumor spread through air spaces (detached clusters in the alveolar spaces); endo-alveolar (intra-alveolar growing underneath a layer of hyperplastic pneumocytes with or without pneumocyte inclusions); and alveolar destructive. These features were compared with histologic features (keratinization, necrosis and cavitation, lymphoid and neutrophilic infiltrates, elastosis, desmoplasia, and large vessel invasion) and the presence of lymph node metastasis.

Results: Thirty-six tumors (35%) had no evidence of alveolar growth; 35 (34%) showed evidence of endoalveolar spread, 22 also with intra-alveolar growth; 25 (24%) had areas of intra-alveolar growth at the periphery without endoalveolar spread; and 7 had areas of tumor spread through air spaces (7%), 5 with either endoalveolar or alveolar growth. Of the 67 tumors with any type of alveolar growth, 40 had some destructive patterns peripherally (59%). Destructive borders were associated with keratinization ($P = .01$), and alveolar spread was associated with increased mitotic figures ($P = .03$). There was no correlation with other histologic features or lymph node status.

Conclusions: A high proportion of squamous carcinomas have advancing edges with alveolar preservation that often overlap with destructive infiltrative growth. Alveolar preservation at the advancing edge is associated with high mitotic rate and absence of keratinization.

Comparison of Programmed Death Ligand 1 (PD-L1) Expression Between Paired Cytologic and Histologic Specimens From Non–Small Cell Lung Cancer Patients

C. Kümpers[1]; L. I. S. van der Linde[3,4]; M. Reischl[5]; W. Vogel[1,2]; F. Stellmacher[2]; M. Reck[3,4]; D. Heigener[4,6]; K. F. Rabe[3,4]; J. Kirfel[1]; L. Welker[3,4]; S. Perner.[1,2] [1]Institute of Pathology, University Hospital Schleswig-Holstein, Campus Lübeck, Lübeck, Germany; [2]Pathology, Research Center Borstel, Leibniz Lung Center, Borstel, Germany; [3]LungenClinic Grosshansdorf, Grosshansdorf, Germany; [4]Airway Research Center North (ARCN), German Center for Lung Research (DZL); [5]Institute for Automation and Applied Informatics, Karlsruhe Institute of Technology, Karlsruhe, Germany; [6]Helios Klinikum Schleswig, Schleswig, Germany.

Context: Expression of programmed death ligand-1 (PD-L1) assessed by immunohistochemistry on histologic samples is a suitable predictive biomarker for identifying patients to benefit from anti–PD-1 immunotherapy. So far, PD-L1 assays are not approved for immunocytochemistry, although a huge portion of non–small cell lung cancer patients are diagnosed solely based on cytologic specimens. The aim of this study was to find out if assessment of PD-L1 expression on cytologic material is feasible and, if so, if PD-L1 expression shows comparable results on paired cytologic and histologic tumor specimens.

Design: Two hundred forty-seven paired samples of non–small cell lung cancer were stained with an anti–PD-L1 antibody and the percentage of PD-L1–positive tumor cells was evaluated by 3 independent investigators. Samples were compared on the basis of the continuous values of PD-L1 expression (ie, values from 0% to 100%) and also categorized with the tumor proportion score as negative (<1%), weakly positive (≥1% to <50 %), or highly positive (≥50%). Concordance was defined if continuous values of paired samples were both within a deviation of 10% and if categorized values were identically grouped.

Results: Based on continuous values between paired samples, a perfect concordance rate was approximately 53%. With categorization of PD-L1 expression based on tumor proportion score, the category was identical in 74.1%. However, defining the continuous values of PD-L1 expression between paired samples within a deviation of 10% as concordant, the concordance rate was 82%.

Conclusions: Evaluation of PD-L1 expression in paired histologic and cytologic tumor specimens shows comparable results if a deviation of 10% between the values is tolerated.

Identifying Immune Infiltration Pattern of Programmed Death Ligand-1 (PD-L1) Positive and Negative Lung Adenocarcinoma

Christiane Kümpers[1]; Mladen Jokic[1]; Carsten Heidel[1]; Anke Fähnrich[3]; Wenzel Vogel[1,2]; Ignacija Vlasic[1]; Jutta Kirfel[1]; Hauke Busch[3]; Sven Perner.[1,2] [1]Institute of Pathology, University Hospital Schleswig-

Holstein, Campus Lübeck, Lübeck, Germany; [2]Pathology, Research Center Borstel, Leibniz Lung Center, Borstel, Germany; [3]Institute of Experimental Dermatology, University of Lübeck, Lübeck, Germany.

Context: There is an urge to characterize mechanisms of tumor immune infiltration based on tumor PD-L1 expression. We aim to identify specific transcriptomic patterns that correspond to immune cell infiltration in lung adenocarcinoma taking into account tumor PD-L1 positivity and total tumor immune cell infiltration. In this manner, we aim to investigate whether tumor immune cell infiltration specificity depends on tumor PD-L1 expression.

Design: PD-L1 expression of 142 lung adenocarcinomas was assessed. Samples were divided into PD-L1–positive and PD-L1–negative groups and were further grouped according to immune cell infiltration into hot tumors and cold tumors. In this way, we assembled 4 groups of cases (PD-L1–positive and hot, PD-L1–positive and cold, PD-L1–negative and hot, and PD-L1–negative and cold), which were analyzed for differential expression of 770 genes covering 24 different immune cells by the NanoString nCounter PanCancer Immune Profiling Panel analysis (NanoString, Seattle, Washington).

Results: PD-L1–positive tumors were significantly more infiltrated by immune cells than their PD-L1–negative counterparts. Furthermore, PD-L1–positive tumors attract more cytotoxic $CD8^+$ lymphocytes than their PD-L1–negative counterparts, but only when heavily infiltrated (hot). Next steps include transcriptomic profiling of defined groups for genes identifying a panel of infiltrating immune cells.

Conclusions: The distribution of total immunologic "hotness" depends on PD-L1 status in lung adenocarcinoma. Tumors expressing PD-L1 also attract more $CD8^+$ lymphocytes than their PD-L1–negative but also heavily infiltrated counterparts. Upcoming experiments will reveal whether PD-L1 expression selects for the specific tumor infiltration pattern.

Programmed Death Ligand-1 Expression in Pulmonary Neuroendocrine Tumors

Deepali Jain[1]; Prerna Guleria[1]; Prabhat Malik[2]; Sunil Kumar[3]; Anant Mohan.[4] Departments of [1]Pathology, [2]Medical Oncology, [3]Surgical Oncology, and [4]Pulmonary Medicine, All India Institute of Medical Sciences, New Delhi, India.

Context: Lung carcinoids differ from high-grade neuroendocrine tumors (NETs) in their biology and behavior. Immunotherapy for high-grade NET is included in recent National Comprehensive Cancer Network guidelines. Detection of programmed death ligand-1 (PD-L1) expression by immunohistochemistry has made easy identification of patients eligible for immunotherapy. We aimed to ascertain expression of PD-L1 on NET lung.

Design: Seventy-five consecutive cases of pulmonary NET were reviewed. Immune cells (ICs) were graded absent, weak (mild, patchy inflammatory cells), moderate (prominent bandlike reaction) or severe (florid inflammation) depending on amount and distribution. Immunohistochemistry for PD-L1 (clone SP263) was performed. Any amount of membranous staining of >1% tumor cells at any intensity was considered positive. Percentage of ICs expressing PD-L1 was also calculated.

Results: Of 75 cases, 1 was typical carcinoid, 5 were atypical carcinoid, 54 were small cell carcinoma, 11 were large cell neuroendocrine carcinoma, and 4 were combined small cell carcinoma. ICs were present in 64.4% of cases (32.9% weak, 26% moderate, 5.5% severe inflammation). PD-L1 on tumor cells was negative in 91.8% of cases. All 6 positive cases (8.2%) were neuroendocrine carcinomas. There were 35.6% of cases with PD-L1 positive IC, which included 40% atypical carcinoid, 30.2% small cell carcinoma, 50% large cell neuroendocrine carcinoma, and 75% (3 of 4) combined small cell carcinoma.

Conclusions: High-grade NETs of lung demonstrate PD-L1 positivity in lower percentages. Carcinoids remain devoid of such expression. PD-L1–positive ICs outnumber tumor cells. Therefore, better response to immunotherapy may be expected in them. NETs of lung possibly represent an immune-privileged group of tumors, thereby a good target for immunotherapy.

Histologic Subtype, Nuclear Grade, and Necrosis in Malignant Mesothelioma: A Comparison of Metastatic to Primary Site

J. Schulte; A. Husain; J. Mueller. Department of Pathology, University of Chicago, Chicago, Illinois.

Context: A metastatic site (MET) may be the first diagnostic specimen in malignant mesothelioma (MM). Pathologic parameters are important in determining prognosis and may direct treatment. This study correlates these parameters between MET and primary sites.

Design: Paired MM with MET and primary sites, pathology reports and hematoxylin-eosin sections were reviewed for histologic subtype. In epithelioid MM, nuclear grade (NG) and necrosis were determined in a blinded fashion.

Results: Twenty-five cases were identified. All MET were E subtype. Positive predictive value of MET epithelioid subtype was 52% (subtype primary site: 13 epithelioid, 12 biphasic, 0 sarcomatoid). Twelve pairs of MET and primaries with epithelioid morphology were graded. Two of 5 (40%) of MET NG1 showed NG1 at primary; NG2 and NG3 showed 100% correlation between MET and primary (κ of NG1, NG2, and NG3 was 0.43, 0.38, and 1, respectively). One of 6 NG1 and 11 of 18 NG2/NG3 at MET had biphasic tumor at primary site, showing that higher grade at MET is more likely to represent biphasic at primary ($P = .003$). Presence or absence of necrosis at MET did not agree with presence or absence of necrosis at primary (κ of 0.05 and 0.35, respectively).

Conclusions: In this retrospective and limited study, there appears to be no clinically significant correlation between MET and primary MM. The metastases from all biphasic tumors were epithelioid. NG and necrosis did not correlate, either; however, an epithelioid tumor with higher NG in MET was more likely to come from a biphasic MM.

Mismatch Repair Proteins and Immunogenic Microenvironment Predict Outcome and Increased Expression of PD-L1 in Malignant Mesothelioma

M. Balancin[1,2]; A. Roden[3]; V. Capelozzi.[1] [1]Department of Pathology, Faculty of Medicine, University of São Paulo, São Paulo, Brazil; [2]Pathology Division, Hospital das Clinicas, Faculty of Medicine, University of São Paulo, São Paulo, Brazil; [3]Department of Laboratory Medicine and Pathology, Mayo Clinic, Rochester, Minnesota.

Context: Tumor growth and invasion involves modulation of mismatch repair (MMR) proteins, immunogenicity, and collagen fibers. Malignant mesothelioma (MM) has been associated with autoimmune responses to asbestos that have been shown to induce collagen production in cultured mesothelial cells. Autoantibodies to type V collagen (Col V) have been identified as a significant risk factor for invasion in cancer. We hypothesized that the cross talk between MMR proteins and immunogenicity promotes a cold-hot microenvironment that acts as a barrier protecting neoplastic cells from chemotherapeutic agents and checkpoint inhibitors.

Design: Ninety-two patients underwent surgical resection for MM in pleura (n = 68), peritoneum (n = 20) and testis (n = 4). Expression of Col V, programmed death ligand-1 (PD-L1, clone SP263), BAP1, MMR proteins, CD4, CD8, and CD20 was quantified by image analysis.

Results: The Table summarizes the significant associations of MMR proteins with morphologic, immune cells, BAP-1, PD-L1 (MC), PD-L1 (TILs), and Col V variables. Cox regression model predicted high risk of death for MM with necrosis ($P = .004$), high nuclear grade ($P = .001$), low MCs-PD-L1 ($P = .07$), loss of BAP1 expression ($P = .005$), low $CD4^+$ ($P = .008$), increased expression of MLH1 ($P = .002$) and MSH2 ($P = .01$), and high Col V fibers ($P = .004$). Both pleural and peritoneal MM expressed similar biomarkers and risk of death profile.

Conclusions: Our findings suggest that PD-L1 depends on the cross talk between Col V and tumor mutation burden to promote tumor necrosis and cold-hot immunogenic switching and to predict death and increased expression of PD-L1 by tumor cells in MM.

Association of MMR Proteins With Morphologic, Immune Cell, BAP-1, PD-L1, and Col V Variables[a]					
Variables	MLH1 (mean, 713/mm²)	PMS2 (mean, 957/mm²)	MSH2 (mean, 1306/mm²)	MSH6 (mean, 855/mm²)	Epithelioid MM (n = 85)
Epithelioid MM (n = 85)	$P = .03$	$P = .04$	$P = .06$	$P = .08$	
Nuclear grade (score 3, n = 23)	$P = .60$	$P = .73$	$P = .84$	$P = .65$	$P = .11$
Necrosis (score 3, n = 18)[b]	$P = .06$	$P = .03$	$P = .07$	$P = .06$	$P = .41$
$CD4^+$ (mean, 60/mm²)	$R = -0.05$	$R = 0.26$	$R = -0.02$	$R = 0.02$	$P = .84$
	$P = .63$	$P = .01$	$P = .83$	$P = .79$	
$CD8^+$ (mean, 301/mm²)	$R = 0.13$	$R = 0.18$	$R = 0.15$	$R = 0.20$	$P = .47$
	$P = .22$	$P = .08$	$P = .15$	$P = .07$	
$CD20^+$ (mean, 186/mm²)	$R = -0.09$	$R = -0.11$	$R = -0.08$	$R = -0.24$	$P = .46$
	$P = .37$	$P = .30$	$P = .42$	$P = .01$	
Col V fibers (mean, 2.67/mm³)	$R = 0.30$	$R = 0.45$	$R = 0.32$	$R = 0.33$	$P = .94$
	$P = .01$	$P = .001$	$P = .006$	$P = .004$	
BAP-1 loss (n = 61, 59%)	$P = .40$	$P = .04$	$P = .05$	$P = .11$	$P = .44$
PD-L1 $(MC)^+$ (mean, 7%)	$P = .01$	$P = .007$	$P = .04$	$P = .009$	$P = .24$
PD-L1 $(TILs)^+$ (mean, 2.94/mm²)	$R = 0.16$	$R = 0.03$	$R = 0.14$	$R = 0.12$	$P = .77$
	$P = .13$	$P = .76$	$P = .17$	$P = .24$	

Abbreviations: Col V, Type V collagen; PD-L1 (MC), PD-L1 on malignant cells (MC); PD-L1 (TILs), PD-L1 on inflammatory cells.
[a]Pearson correlation except as noted; R = coefficient of correlation; P value = significance $< .05$.
[b]Spearman correlation.

HEG1 Is Useful for Cytologic Diagnosis of Malignant Mesothelioma With Serosal Effusions

K. Hiroshima[1]; D. Wu[1]; D. Ozaki[2]; M. Hasegawa[3]; E. Koh[4]; Y. Sekine[4]; S. Tsuruoka[5]; S. Hamakawa[6]; K. Nabeshima[7]; S. Tsuji[8]; Y. Miyagi[8]; K. Imai.[9] [1]Department of Pathology, Tokyo Women's Medical University, Yachiyo Medical Center, Yachiyo, Japan; [2]Department of Pathology, Chiba Rosai Hospital, Ichihara, Japan; Departments of [3]Respiratory Medicine and [4]Thoracic Surgery, Tokyo Women's Medical University, Yachiyo Medical Center, Yachiyo, Japan; [5]Department of Pathology, Saitama Medical Center, Saitama, Japan; [6]Department of Pathology, Showa General Hospital, Kodaira, Japan; [7]Department of Pathology, Fukuoka University Hospital and School of Medicine, Fukuoka, Japan; [8]Kanagawa Cancer Center Research Institute, Yokohama, Japan; [9]The Institute of Medical Science, The University of Tokyo, Tokyo, Japan.

Context: HEG1 has been proposed as a positive mesothelial marker. Cytologic diagnosis of mesothelioma in serosal effusions is based on immunohistochemistry and ancillary techniques.

Design: Cell blocks including 42 mesotheliomas, 33 with reactive mesothelial cells (RMCs), 19 lung carcinomas, 12 ovarian carcinomas, 7 other carcinomas, and 1 angiosarcoma were analyzed immunohistochemically with HEG1. Cell blocks from mesotheliomas and RMCs were also analyzed with BAP1, MTAP, and *p16* fluorescence in situ hybridization (FISH).

Results: All mesotheliomas showed HEG1 expression and most of them showed membranous staining. All RMCs, 6 of 12 ovarian carcinomas (50.0%), and 1 angiosarcoma showed HEG1 expression. Lung carcinomas and other carcinomas did not express HEG1. Expression rates of calretinin, WT1, and D2-40 in cell blocks of mesotheliomas analyzed were 89.3%, 92.6%, and 90.0%. HEG1 can detect mesothelioma with 100% sensitivity and 82.1% specificity on cytologic specimens. Thirty of the 39 mesotheliomas (76.9%) evaluated by FISH showed homozygous deletion of *p16*, but RMCs did not. Loss of BAP1 and MTAP was found in 73.0% (27 of 37) and 86.7% (13 of 15) of mesotheliomas, respectively, but in none of RMCs. There was concordance between loss of MTAP staining and deletion of *p16* by FISH in 15 of 16 evaluable cases (93.8%).

Conclusions: Mesotheliomas identified in serosal effusion specimens expressed HEG1, whereas lung carcinomas were negative. Deletion of *p16* by FISH is observed frequently in serosal effusions positive for mesothelioma, and MTAP immunohistochemistry can be a surrogate for *p16* FISH.

Preoperative Bronchial Cytology Samples Do Not Adequately Predict the Presence of Tumor Spread Through Airspaces in Resected Lung Adenocarcinoma

M. Medina[1]; A. Onken[1]; Y. Chen[1]; C. de Margerie-Mellon[2]; A. Bankier[2]; P. VanderLaan.[1] Departments of [1]Pathology and [2]Radiology, Beth Israel Deaconess Medical Center and Harvard Medical School, Boston, Massachusetts.

Context: Bronchoscopic procedures are frequently used for the diagnosis of lung cancer, often including bronchoalveolar lavage (BAL) and bronchial washing (BW) cytology specimens. Tumor spread through air spaces (STAS) is a significant prognostic finding in resected lung carcinomas. However, to date, there is limited ability to predict STAS prior to surgery.

Design: To determine if BAL/BW specimens are predictive of STAS, we evaluated all resected lung adenocarcinomas at our institution from 2008 to 2018 that had an antecedent bronchoscopy with BAL/BW (N = 74). The BAL/BW cytology slides were reviewed and categorized as either positive or negative for carcinoma, and the corresponding surgical resection specimens were separately evaluated for the presence of STAS. Other clinical, radiologic, and pathologic features of the resection specimens were also evaluated. Chi-square test and univariate/multivariate logistic regression models were used to assess statistical significance.

Results: Positive BAL/BW cytology was observed in 29 cases (39.2%), 24 of which were positive for STAS (82.8%); however, negative BAL/BW cytology was observed in 45 cases (60.8%), 34 of which were positive for STAS (75.6%) (Table; $\chi^2 = 0.54$, $P = .46$, not significant). Of all the other assessed clinicopathologic and radiologic features, the only statistically significant association found by logistic regression for BAL/BW positivity was with visceral pleural invasion.

Conclusions: Preoperative bronchial cytology cannot predict STAS, though it does appear to correlate with visceral pleural invasion. These findings have further indirect implications for the nature of STAS, as well as the ability to predict its presence prior to surgery.

Preoperative Bronchial Cytology and STAS			
	STAS Absent	STAS Present	Total
BAL/BW negative	11	34	**45**
BAL/BW positive	5	24	**29**
Total	**16**	**58**	**74**

A Year of Nonconformance With American Joint Committee on Cancer 8th Edition TNM Guidelines for Lung Cancer Staging

B. McGovern; S. Nicholson. Department of Histopathology, St James's Hospital, Dublin, Ireland.

Context: Our lung group adopted the 8th edition of the American Joint Committee on Cancer (AJCC) TNM cancer staging system in January 2017. For invasive lung adenocarcinoma, this edition dictates that tumor size be determined by the largest dimension of solid portion (clinical) or by invasive portion (pathologic). However, we use whole tumor size because of difficulty in distinguishing lepidic from invasive growth.

Design: After 1 year (2017), we recalculated tumor size and group stage based on invasive tumor in resected lung adenocarcinomas and reviewed clinical significance. Pathology reports for invasive lung adenocarcinomas resected in 2017 were reviewed for whole tumor size, growth pattern percentages, TNM, and group stage. Invasive tumor size was calculated by multiplying the whole tumor size by the percentage invasion. pT and group stage were reassigned using invasive tumor as pT.

Results: There were 271 lung resections. Eighty-six were invasive lung adenocarcinomas, 36 with a lepidic component, thus having different invasive and total tumor sizes. Size difference ranged from 1 to 26 mm, with an average of 8.3 mm. Substituting total tumor size with invasive size had no impact on pT in 19 cases because of minimal size difference or other factors: pleural invasion (pT2a), ipsilateral satellite tumor nodules (pT3), or mediastinal invasion (pT4). Substituting total with invasive size altered pT in 17 cases. Group stage was unchanged in 3 of 17 because of nodal metastasis. Group stage changed in 14 cases: 3 downstaged from II to I, and 11 downstaged within stage I.

Conclusions: The AJCC 8th edition ignores the issue of distinguishing lepidic from invasive growth. Invasive tumor size was downstaged in 16% of our cases.

A Rare Case of Lung Adenocarcinoma In Situ With Intratumoral Sarcoidlike Granuloma (SLG)

Reishi Seki[1]; Kenshiro Omura[2]; Shoji Kuriyama[2]; Masahiro Kaji.[2] Departments of [1]Diagnostic Pathology and [2]Thoracic Surgery, Tokyo Saiseikai Central Hospital, Japan.

Malignant tumors often develop noncaseating epithelioid granuloma, which is recognized to be caused by soluble tumor antigens via necrotic cells or T cells. This granuloma is widely reported in Hodgkin lymphoma and is considered to be a good prognostic factor, occurring in approximately 4.4% of various carcinomas. In lung carcinoma, SLG is often found in the mediastinal lymph nodes as well as the tissue around the tumor, and there are few reports showing its existence within the tumor. Here, we report a rare case of lung adenocarcinoma in situ with intratumoral SLG. This case was a 70-year-old man with a history of right nephrectomy because of renal cell carcinoma 1 year previous. During the follow-up period, his chest computed tomography showed a part-solid ground-glass nodule (20 mm in size) in the right middle lobe, resulting in middle-lobe lobectomy (Figure 3, A and B). Histologically, colonization of small noncaseating epithelioid granuloma was found in the central part of the nodule consisting of adenocarcinoma in situ (Figure 3, C and D). No apparent destruction of the alveolar wall due to the tumor was found, leading to the diagnosis of lung adenocarcinoma in situ with intratumoral SLG. SLG was also found in the dissected mediastinal lymph nodes. In contrast, SLG was not found in the prior resected specimens of renal cell carcinoma. To date, cases of intratumoral SLG in lung cancer have been rarely reported as compared with those in renal cell carcinoma.

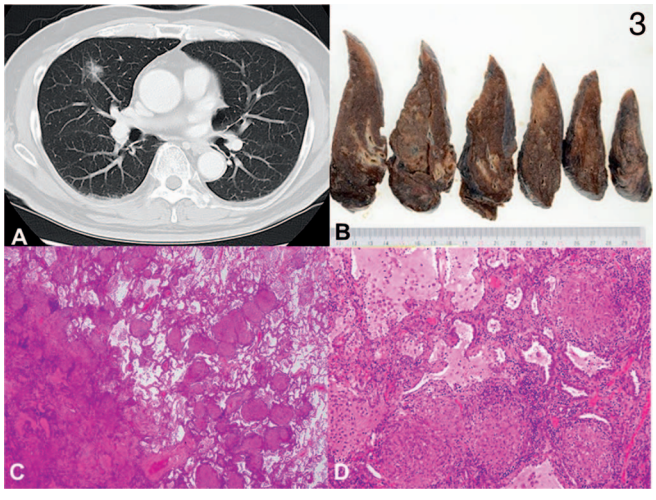

An Unusual Presentation of a Recently Described Rare Lung Tumor

S. Jogai. Department of Cellular Pathology, University Hospital Southampton, Southampton, United Kingdom.

A 58-year-old man presented with progressive shortness of breath with clinical and imaging features consistent with sarcoidosis. Bronchial biopsy showed a proliferation of small, relatively bland cells positive with only synaptophysin. Taking into account the imaging, the possibility of diffuse idiopathic pulmonary neuroendocrine cell hyperplasia was raised. Further imaging showed enlarged mediastinal nodes and features suspicious of bone involvement. Mediastinal lymph node biopsy showed involvement by similar tumor cells; these were synaptophysin positive but other neuroendocrine as well as epithelial, mesothelioma, melanoma, and germ cell markers were negative. Cytogenetics showed no rearrangement of *SS18* or *EWSR1*. The patient was treated with palliative chemotherapy for metastatic carcinoma of unknown primary. A year later, he presented with progressive disease. A left upper lobe biopsy showed variable patterns: spindle cells in fascicles, sclerotic stroma, hob nailing, rare mitoses, but no necrosis. The features were suspicious of a vascular tumor, but the tumor cells were CD34, CD31, and factor VIII negative. Expert opinion from Mayo Clinic reported this as a composite hemangioendothelioma with neuroendocrine marker expression. These are extraordinarily rare endothelial tumors of intermediate malignancy. They show neuroendocrine marker expression rather than neuroendocrine differentiation, with only synaptophysin expressed and no expression of chromogranin. It is likely that that bone was the primary site. The important take-home message from this case is that interpretation of immunohistochemistry is crucial; awareness of aberrant expression of synaptophysin in this type of tumor was crucial to the correct diagnosis and that synaptophysin expression does not equate with neuroendocrine differentiation.

ROS1 Translocation Relates With TTF1 and Vimentin Expression in Pulmonary Adenocarcinomas

M. R. Silva[1,2,3]; A. Alarcão[1,2,3]; A. Ladeirinha[1,2]; T. Ferreira[1,2]; A. Rodrigues[1], V. Sousa[1,2,3,4]; L. Carvalho.[1,2,3,4] [1]Institute of Anatomical and Molecular Pathology, [2]CIMAGO Research Center for Environment, Genetics and Oncobiology, and [3]Centre of Pulmonology, Faculty of Medicine, University of Coimbra, Coimbra, Portugal; [4]University Hospital Anatomical Pathology, Coimbra, Portugal.

Context: Mutated *EGFR, ALK,* and *ROS1* tyrosine kinase receptors, among others, help to determine patients eligible for therapy for pulmonary adenocarcinoma, which are associated with higher survival. Crizotinib has been approved as a first-line therapy for patients expressing *ROS1* translocation. Vimentin expression of malignant epithelial cells has been correlated with epithelial to mesenchymal transition (EMT) activation carcinogenesis, which is associated with poor prognosis.

Design: Seven patients older than 60 years old (5 men and 2 women) with $ROS1^{+}$ adenocarcinomas treated with crizotinib were studied. Biopsies (3 bronchial, 4 transthoracic) were evaluated by immunohistochemistry for CK7, TTF1, CK5.6, vimentin, CDX2, CD56, and PD-L1 (22C3, Dako) performed on a BOND-MAX (Leica) platform. Fluorescence in situ hybridization with ZytoLight SPEC *ROS1* (ZytoVision, Bremerhaven, Germany) probe was scored: ROS1-positive pattern with fused and split signals, or one fusion signal and isolated green signals >15% neoplastic cells.

Results: The *ROS1*-translocated adenocarcinomas had the triad expression of CK7/TTF1/vimentin in common; they were negative for CDX2/CK5.6/CD56. PD-L1 22C3 Dako expression was greater than 50% in cases 3 and 5; case 6 had 2% positive cells and the other cases were negative. Four patients were alive 18 months after beginning therapy.

Conclusion: Specimen type did not influence/exclude immunohistochemistry studies including TTF1/vimentin and PD-L1 determination followed by *ROS1*-positive testing and *EGFR* and *ALK* testing in 7 patients. This small series of surviving adenocarcinoma patients with

EMT carcinogenesis prognosis might suggest vimentin beyond TTF1 to be included in pathology reports, apparently with *ROS1* relationship.

Programmed Death Ligand 1 (PD-L1) Heterogeneity Expression in Biopsy: Reporting Difficulties

Vitor Sousa[1,2,3,5]; Ana Alarcão[1,2,3]; Ana Filipa Ladeirinha[1,2]; Ines Figueiredo[1]; Maria Reis Silva[1,2,3]; Teresa Ferreira[1,2]; Ana Isabel Rodrigues[1]; Lina Carvalho.[1,2,3,5] [1]Institute of Anatomical and Molecular Pathology, [2]CIMAGO Research Center for Environment, Genetics and Oncobiology, and [3]Centre of Pulmonology, Faculty of Medicine, University of Coimbra, Coimbra, Portugal; [4]Internal Medicine, University Hospital Coimbra, Portugal; [5]University Hospital Anatomical Pathology, Coimbra, Portugal.

Context: The treatment of lung carcinoma has significantly changed in the decade, resulting in improved survival in patients treated with monoclonal antibodies and inhibitors targeting mutated/amplified growth factor receptors as well as programmed-death blockage. Antibodies blocking programmed death 1/PD-L1 interaction currently support therapy decisions dependent on/validated by tumoral cell/stromal cell–lymphocyte immunohistochemical expression. Scoring and interpretation of PD-L1 expression is challenging. Here we report 2 cases with challenging interpretation of PD-L1 (22C3, Dako, Lisboa, Portugal) assay.

Design: Case 1 was a 58-year-old man with right upper lobe tumor transthoracic biopsy showing adenocarcinoma with solid, acinar, and papillary patterns in fibro-lymphocytic stroma and expression of CK7, TTF1, and vimentin. Case 2 was a 57-year-old man with right upper lobe tumor biopsy showing mucinous and solid adenocarcinoma in predominant fusiform stroma with TTF1/CK7 expression and negative vimentin. PD-L1 (22C3, Dako) immunostain was performed on a Ventana platform (Roche, Lisboa, Portugal) and the slides were evaluated by 2 trained pathologists.

Results: (1) PD-L1 complete/incomplete linear cytoplasmic membrane expression was observed in 35% of tumor cells. No staining was observed in acinar/papillary patterns, but the original report stated 100% expression referring to solid patterns. (2) PD-L1 complete/incomplete linear cytoplasmic membrane expression was reported in 30% of the PAS^+ tumor cells admixed with predominantly PAS^- large cells.

Conclusions: PD-L1 expression in more than 50% of tumor cells might be limited to a specific adenocarcinoma pattern/cell type, frequently solid subtype. Heterogeneity of PD-L1 expression might be reported because of the potential impact on treatment response.

Utility of Programmed Cell Death Ligand-1 (PD-L1)/CD8 Dual Immunohistochemistry (dIHC) in Predicting Response to Immunotherapy in Lung Cancer

M. Rosenbaum[1]; J. Gainor[2]; M. Mino-Kenudson.[1] [1]Department of Pathology and [2]Cancer Center of Massachusetts General Hospital, Boston.

Context: Programmed death ligand-1 (PD-L1) immunohistochemistry is imperfect for predicting response to PD-1/PD-L1 blockade (PD-B). We used PD-L1/CD8 dual immunohistochemistry (dIHC) in 2 cohorts of non–small cell lung cancer to see if $CD8^+$ tumor-infiltrating lymphocytes (TILs) and stromal cells may help predict PD-B response.

Design: Patients who received PD-B were identified from oncology databases. The first cohort received nivolumab as a second- or later-line treatment. Tissue samples were mainly obtained before initial therapy. The second cohort received first-line pembrolizumab, and tissue samples were procured immediately before PD-B. PD-L1/CD8 dIHC was used to calculate PD-L1 tumor proportion score and semiquantitatively assess $CD8^+$ TILs/stromal cells.

Results: There were 50 patients in the nivolumab and 27 in the pembrolizumab cohort. In the nivolumab cohort, PD-L1 tumor proportion score and $CD8^+$ TILs/stromal cells were unassociated with response rate or progression-free survival. A subset of patients with tumor proportion score >1% and high $CD8^+$ stromal/TILs had reduced progression-free survival ($P = .03$). In the pembrolizumab cohort, all cases exhibited PD-L1 tumor proportion score ≥50%. High $CD8^+$ TILs, high stromal T cells, and both were correlated with improved progression-free survival ($P = .03$, $P = .02$, and $P = .004$, respectively). High $CD8^+$ stromal cells and high stromal/TILs were associated with improved overall survival ($P = .02$ and $P = .03$, respectively).

Conclusions: Increased $CD8^+$ TILs and stromal cells were associated with improved patient outcomes. dIHC on pre–initial treatment samples was less informative but identified a subset of poor responders to later-line PD-B. These results suggest that PD-L1/CD8 dIHC may be useful for predicting response to PD-B in advanced non–small cell lung cancer patients.

Can Large Cell Neuroendocrine Carcinomas of the Lung Be Subdivided Using the Pancreatic Neuroendocrine Criteria?

R. E. Fanaroff; K. M. Stashek; A. P. Burke. Department of Pathology, University of Maryland Medical Center, Baltimore.

Context: Neuroendocrine tumors (NETs) of the lung are classified as carcinoid, atypical carcinoid, large cell neuroendocrine carcinoma, and small cell carcinoma. Gastrointestinal (GI) NETs, particularly of the pancreas, have been reclassified as well-differentiated NET grades 1 through 3 and poorly differentiated, large cell and small cell. The purpose of this study is to determine if a similar reclassification may be applied to the lung, emphasizing the division of large cell neuroendocrine carcinomas between well-differentiated grade 3 NETs and poorly differentiated neuroendocrine carcinomas, large cell type.

Design: Evaluation was retrospectively performed on tumors diagnosed as large cell neuroendocrine carcinomas from 2003 to the present (N = 36). Carcinoids, atypical carcinoids, and small cell carcinomas were excluded. Evaluation was performed by a pathologist specialized in GI neuroendocrine tumors. One routine-stained slide was reviewed per case to evaluate nested/organoid architecture, trabecular architecture, regular intratumoral vascular pattern, abundant granular cytoplasm, and stippled nuclei with inconspicuous nucleoli. Each parameter was given a score of 0 (absent), 0.5 (focal), or 1 (present). A score of <2 was diagnosed as poorly differentiated neuroendocrine carcinoma, large cell type, and >3 well-differentiated NET grade 3, with the remainder ambiguous.

Results: Patterns identified were organoid growth (score 18), abundant cytoplasm (10.5), trabecular growth (7.5), stippled nuclei (6.5), and vascular pattern (2). Twenty-six tumors were classified as large cell neuroendocrine carcinomas, 8 as ambiguous, and 2 as well-differentiated NET grade 3.

Conclusions: Most tumors were classified as poorly differentiated neuroendocrine carcinomas, large cell type, by gastrointestinal criteria. Further study is required to confirm the validity of the subclassification for lung NECs.

Clinicopathologic Significance of Neuroendocrine Differentiation, p53 Aberrant Expression, and Loss of Rb Expression in Lung Adenocarcinomas

Y. Hung; M. Kem; M. Mino-Kenudson. Department of Pathology, Massachusetts General Hospital and Harvard Medical School, Boston.

Context: A subset of non–small cell lung carcinomas expresses neuroendocrine (NE) markers despite lacking histologic evidence of NE features. This study examined the significance of NE markers, p53, and Rb expression in lung adenocarcinomas (LUAD).

Design: In a cohort of 346 LUAD (including 260 with outcome data), we performed immunohistochemistry on tissue microarray sections for synaptophysin, chromogranin, CD56, Rb, and p53.

Results: In this cohort (218 female, 128 male; median age 69 years; 79% smokers; 77% stage 1; 57% tumors acinar/lepidic-predominant), positivity for 1 NE marker was detected in 24 (7%), 2 markers in 4 (1%), and all 3 markers in 2 (0.6%). Synaptophysin and/or CD56 expression was considerable (≥25%) in 12 tumors. NE marker expression alone was not associated with any clinicopathologic features, *KRAS*/*EGFR* mutation status, or p53/Rb expression. Aberrant p53 expression was seen in 45% of LUAD, more prevalent in solid-predominant adenocarcinoma than other subtypes (68% versus 44%; $P < .01$) and in *KRAS*–wild-type than *KRAS*-mutant tumors (55% versus 37%; $P < .01$). Rb loss was seen in 19% of LUAD, more common in *EGFR*-mutant than *EGFR*–wild-type tumors (35% versus 14%; $P < .002$). No prognostic significance was noted with any NE immunoreactivity or aberrant p53/Rb expression. Subgroup analysis showed considerable (≥25%) NE marker expression associated with worse overall survival ($P < .05$), including those with stage 1 disease ($P < .05$).

Conclusions: NE differentiation by immunohistochemistry, aberrant p53 expression, and loss of Rb expression were each present in a fraction of LUAD. Although focal NE immunoreactivity and aberrant p53/Rb expression carried no prognostic significance, considerable NE expression portended poor prognosis.

Bronchiolocentric Interstitial Pneumonia as a Histologic Pattern of Familial Interstitial Pneumonia

A. T. Fabro[1]; A. B. Hortense[2]; S. S. Batah[1]; J. A. Baddini-Martinez.[2] [1]Department of Pathology and Medicine Legal, and [2]Internal Medicine Department, Ribeirão Preto Medical School, University of São Paulo, São Paulo, Brazil.

Context: Familial interstitial pneumonia (FIP) is defined by the presence of at least 2 cases of fibrosing lung disease within the same biological family. As the interaction of multiple factors, such as genetic and environmental, contributes to the phenotype of an affected individual, our aim was to describe the histopathologic pattern of FIP in a selected sample of the Brazilian population.

Design: Between 2014 and 2017, an active search for familial interstitial pneumonia cases was performed and 35 patients were selected. In only 6 cases, the lung biopsy was obtained for a thorough pathologic review.

Results: History of smoking was reported in 45.7% of the cases, and other relevant environmental exposures were reported in 80%. It is relevant to emphasize that a history of bird exposure was present in 57.1% of the individuals. One case exhibited diffuse alveolar damage and organizing pneumonia related to terminal events, due to fatal acute exacerbation or prolonged mechanical ventilation. Another case showed nonclassifiable fibrosing and cellular interstitial pneumonitis. The other 4 cases were defined as bronchiolocentric interstitial pneumonitis, 3 of them with active organizing myofibroblastic centrilobular areas. Of these cases, 2 reported current exposure to birds: one had current exposure to birds and goose feather pillow, and the other had exposure to birds in the past. After multidisciplinary discussion, they were diagnosed as hypersensitivity pneumonitis.

Conclusions: Bronchiolocentric interstitial pneumonitis is an important pattern in cases of familial interstitial pneumonia in Brazil, indicating a complex interaction between environment, genetics, and predisposition to hypersensitivity pneumonitis in the Brazilian population.

Surgical Lung Biopsy by Videothoracoscopic Procedure in Pulmonary Interstitial Disease: Cost-Effectiveness at a Secondary Hospital in Brazil

T. R. Nadai[1,4]; S. S. Batah[2]; M. A. Alda[2]; J. Machado-Rugolo[2]; C. C. I. Cirino[1]; A. A. Neto[1]; L. R. Alves[3]; A. I. Padua[3]; R. G. Felix[2]; F. H. G. Cipriano[4]; L. U. Dessote[4]; M. K. Santos[5]; A. T. Fabro[2]; J. A. Baddini-Martinez.[3] [1]Américo Brasiliense State Hospital, Brazil; [2]Pathology and Legal Medicine, [3]Internal Medicine Department, [4]Division of Thoracic and Cardiovascular Surgery, Department of Surgery and Anatomy, and [5]Center of Imaging Sciences and Medical Physics, Ribeirão Preto Medical School, University of São Paulo, São Paulo, Brazil.

Context: Surgical lung biopsies are important for diagnosis and clinical treatment of interstitial lung diseases, which could be obtained by videothoracoscopic procedures. Our aim was to analyze the clinical, pathologic, and financial results of surgical lung biopsies at Américo Brasiliense secondary hospital.

Design: Retrospective cohort study of surgical lung biopsies by videothoracoscopic procedures performed at Américo Brasiliense State Hospital.

Results: Videothoracoscopic procedures were performed on 45 patients during 24 months. Mean surgical procedure time was 42 minutes. Sixty-one lung lobes were biopsied (31.1% bilobar, 66.7% single lobes); right lower lobe was the most common biopsy site (62.2%) and mean stapler loads were 2.86 per surgery (2–5). The mean time of hospitalization was 3.68 days (1–19). The overall complication rate was 11.11%, including pneumothorax, pleural effusion, prolonged air leak, and pneumonia. No deaths were reported within 90 days. The final diagnoses by multidisciplinary discussion were chronic hypersensitivity pneumonitis (26.6%), aspiration (22.2%), drug-related (17.78%), idiopathic pulmonary fibrosis (8.8%), and sarcoidosis (4.4%). The average cost for the procedure was $1612.00 per patient, which is 3.32 times higher than the cost for other surgical procedures at community hospital.

Conclusions: Videothoracoscopic procedures for interstitial diseases have a high diagnostic sensitivity and few clinical complications. However, the cost per procedure is higher than for other similar surgical procedures, because of the expensive cost of staplers in Brazil. Shorter hospital stays and rapid diagnosis may reduce the overall cost.

A Case of Granulomatous Pneumonia in a Former Drug Abuser

M. Fraig. Department of Pathology and Laboratory Medicine, University of Louisville School of Medicine, Louisville, Kentucky.

The patient is a 29-year-old man who presented to the emergency department for bilateral knee and ankle pain. He complained of night sweats for several weeks and a recent weight loss of 24 pounds in 4 weeks. He denied diarrhea, vomiting, fever, or injury to the knees or joints. He was diagnosed with eosinophilic pneumonia at an outside facility and was admitted there 3 times. He received 2 L of oxygen at baseline in addition to 60 mg of prednisone daily. His laboratory work was significant for low hemoglobin at 11.9 g/dL, increased WBC at 31.7 $\times$ 10^3/mm^3 with 21% eosinophils. His initial chest x-ray was within normal but the second chest x-ray showed bilateral opacities. His respiratory status declined, requiring 15 L of oxygen. Bronchoalveolar lavage showed significant eosinophilia. He underwent a wedge biopsy of the lung that revealed perivascular and parenchymal granulomatous inflammation obliterating blood vessels consistent with possible intravenous drug abuse. The patient reported using cocaine in the past but said he had stopped 3 years prior to his admission. The differential diagnosis included aspiration pneumonia, drug abuse, pneumoconiosis or parasitic infection. The patient recalled that his dog had recently died after suffering bouts of diarrhea. The patient reported that he had received a bite from his dog on his right middle finger. After careful examination, the patient was diagnosed with echinococcal pneumonia. He was started on mebendazole 400 twice daily for 4 weeks. The leukocytosis and eosinophilia improved, and he was saturating at 98% on 2 L of oxygen.

Congenital Diaphragmatic Hernia (CDH)–induced Vascular Lung Remodeling Is Modulated by Transplacental Nitrite

A. T. Fabro[1]; R. L. Figueira[2]; M. V. Alavarse[2]; K. M. Costa[2]; S. S. Batah[1]; P. S. Leão[1]; R. G. Felix[1]; J. E. T. Santos[2]; G. C. Ferreira[2]; L. Sbragia.[2] [1]Pathology and Legal Medicine and [2]Department of Surgery and Anatomy, Ribeirão Preto Medical School, Ribeirão Preto, Brazil.

Context: Nitrite is an alternative nitric oxide (NO) source related to modulating vascular tone and remodeling by downstream signaling pathways of vascular smooth muscle cells. In contrast, the nonfunctional relaxing of lung vessels is a critical feature to understand pathophysiologically the pulmonary hypoplasia of congenital diaphragmatic hernia (CDH). Its lung architectural distortion is induced by dysregulation of the molecular cellular interaction, leading to the primary diaphragm defect and potentially to direct effects on lung development. Our aim was to analyze the experimental efficacy of oral nitrite treatment in modulating the muscularization and the adventitial thickening of pulmonary arterioles in CDH.

Design: Sprague-Dawley pregnant rats were exposed (CDH group) or not (control group) to nitrofen on gestational day 9.5. to induce CDH model. The pregnant rats from the treatment group (CDH + Nit group) received nitrite by gavage (15 mg/kg, 1 ml/kg) on the last 5 gestational days. On gestational day 21.5 the fetuses were harvested. The following parameters were analyzed: lung and plasma NO_2^- levels, medial wall thickness from arterioles between 30 and 60 μm, eNOS and iNOS immunohistochemistry. Statistical analysis was performed using ANOVA with Bonferroni posttest. $P < .05$ was considered significant.

Results: Lung and plasma levels of NO_2^- and eNOS expression levels were recovered in the CDH + Nit group ($P < .05$), medial wall thickness was decreased (vasodilated) in the same group (CDH + Nit) compared with CDH ($P < .05$), and iNOS expression was decreased in the treated groups ($P < .05$).

Conclusions: Nitrite maternal administration rescued the arteriolar morphometry and recovered eNOS expression from CDH lungs in the nitrofen-induced CDH model. Nitrite may be an effective preventive of PH in CDH newborns.

Prominent Airway-Centered Fibroblastic Foci (ACFF) as a Marker of Chronic Microaspiration (CMA)

S. S. Batah[1]; M. A. Alda[1]; P. S. Leao[1]; J. A. Baddini-Martinez[2]; M. Koenigkam-Santos[3]; V. L. Capelozzi[4]; R. Duarte Achcar[5]; A. T. Fabro.[1] [1]Pathology and Legal Medicine, [2]Internal Medicine Department, and [3]Center of Imaging Sciences and Medical Physics, Ribeirão Preto Medical School, University of São Paulo, Brazil; [4]Pathology, Faculty of Medicine, University of São Paulo, Brazil; [5]Department of Medicine, Pathology Division, National Jewish Health, Denver, Colorado.

Context: Chronic microaspiration (CMA) may lead to interstitial inflammation and fibrosis. However, the contribution of CMA to bronchiolocentric interstitial pneumonia with fibrosis (BIPF) is not entirely understood. We hypothesized that CMA may manifest as prominent airway-centered fibroblastic foci (ACFF).

Design: Seventy-one patients diagnosed with BIPF by surgical lung biopsy were evaluated during a 3-year period (2017–2019). After multidisciplinary discussion, 8 patients were diagnosed with hypersensitivity pneumonia, 4 with interstitial pneumonia with autoimmune features, and 4 with CMA. Two authors blindly reviewed all surgical lung biopsies and scored for prominent ACFF. Clinical and demographic data and pulmonary function test results before (1–2 m) and after (8–12 m) surgical lung biopsies were collected from electronic medical records.

Results: The average age of patients was 62 years, and 57% were female. Exposure histories were available in 87% of hypersensitivity pneumonia patients, and evidence of gastroesophageal reflux disease was documented in 100% of CMA patients. Twenty-five percent of CMA patients were diagnosed with probable usual interstitial pneumonia pattern by chest HRCT. Surprisingly, patients with CMA exhibited significantly higher ACFF scores ($P < .05$) and significantly less pronounced decline in diffusing capacity for carbon monoxide than those with hypersensitivity pneumonia and interstitial pneumonia with autoimmune features ($P < .05$).

Conclusions: We demonstrate that prominent ACFF may be seen in BIPF secondary to CMA, which may present with probable usual interstitial pneumonia pattern of fibrosis on image studies, and should be considered in the differential diagnosis of BIPF. BIPF secondary to CMA had a better prognosis compared with hypersensitivity pneumonia and interstitial pneumonia with autoimmune features.

Pathologic Features of Acute Exacerbation of Chronic Interstitial Pneumonia in Autopsy Cohort

T. Tanaka[1]; K. Ishida.[2] [1]Department of Diagnostic Pathology, Kobe University Hospital, Hyogo, Japan; [2]Department of Pathology and Laboratory Medicine, Kansai Medical University, Osaka, Japan.

Context: In chronic interstitial pneumonia (ChIP), acute exacerbation (AEx) is a critical condition directly associated with the cause of death. The detailed pathology of AEx of ChIP is not well understood.

Design: Twenty cases of AEx of ChIP were identified from autopsy archives of Kindai University Hospital. The definition of AEx was according to the American Thoracic Society working group report. Two pathologists retrospectively evaluated the pathologic findings.

Results: Fourteen patients had idiopathic ChIP and 6 had ChIP associated with collagen vascular disease. Sixteen were idiopathic AEx, and 4 were triggered AEx. Subtypes of ChIP were 14 cases usual interstitial pneumonia, 4 cases nonspecific interstitial pneumonia, and 2 cases unclassifiable. Surprisingly, in 11 cases hyaline membranes were rare or absent. Most of the cases (8 of 11) exhibited an organizing phase of diffuse alveolar damage; pulmonary congestion was seen in the remaining 2 cases and pneumonia in 1 case. Eight of 20 demonstrated pulmonary alveolar hemorrhage. In addition, severe pulmonary congestion was observed in 7 cases, and a capillary hemangiomatosis-like change was observed in the alveolar walls. Squamous metaplasia was conspicuously recognized in 5 cases.

Conclusions: The pathologic condition of AEx of ChIP demonstrated more diverse histology than previously considered, and it needs to be examined in more cases in the future.

Pulmonary Alveolar Hemorrhage and Diffuse Alveolar Damage Were Common Causes of Death in Patients With Myelodysplastic Syndrome

K. Ishida[1]; T. Tanaka.[2] [1]Department of Pathology and Laboratory Medicine, Kansai Medical University, Osaka, Japan; [2]Department of Diagnostic Pathology, Kobe University Hospital, Hyogo, Japan.

Context: Myelodysplastic syndrome (MDS) is often complicated with a pulmonary disorder; however, there is little known about the pulmonary pathology associated with MDS. We hypothesized that pulmonary manifestation of MDS may have some common features.

Design: Seventeen patients with MDS were identified from autopsy archives at Kindai University Hospital. Two pathologists retrospectively reviewed the cases in order to identify characteristic histologic findings.

Results: Fifteen of 17 had a pulmonary disorder, 12 of which were associated with the cause of death. Six of 17 progressed to leukemia, 4 of which showed infiltration of leukemic cells in the lung tissue. Ten of 17 demonstrated pulmonary alveolar hemorrhage, 10 had diffuse alveolar damage, and 9 showed organizing pneumonia. The pulmonary alveolar hemorrhage and diffuse alveolar damage were a direct cause of death. Five had pulmonary infection such as fungi. Five showed chronic pulmonary fibrosis, 2 who demonstrated usual interstitial pneumonia pattern, 2 nonspecific interstitial pneumonia pattern, and 1 airspace enlargement with fibrosis.

Conclusions: In this autopsy series of MDS, the pulmonary complications were frequent and directly related to death. It is important to understand the pathogenesis of pulmonary complications in order to elucidate the cause of death of MDS.

Pulmonary Epithelioid Hemangioendothelioma (EHE): Case Report of a Rare Vascular Tumor

A. Elatre; A. Abdelhalim; M. Koss. Department of Pathology, Keck Hospital of University of Southern California, Los Angeles.

A healthy 72-year-old woman with no known comorbidities was admitted for a history of asymptomatic multiple bilateral pulmonary nodules noted as an incidental finding 5 years prior. The patient underwent extensive workup including serial computed tomography and positron emission tomography scans, computed tomography–guided biopsy, and bronchoscopy with biopsy. Histomorphology revealed advancing nodular pattern of growth with fibromyxoid stroma, coagulative central necrosis, and intracytoplasmic vacuoles. Immunohistochemical staining was positive for vascular markers CD34 and CD31 and negative for CK, p63, MOC31, TTF-1 and Congo red stains. EHE is a well-differentiated, rare vascular tumor, with a wide spectrum of behavior and an epithelioid and histiocytoid appearance. It originates from pre-endothelial or vascular endothelial cells, and represents <1% of all vascular neoplasms. The term EHE was first introduced by Weiss et al as a soft tissue vascular tumor of borderline malignancy. However, the lesion was originally described in 1975 by Dail et al as an intravascular bronchoalveolar tumor, initially believed to be an aggressive form of the bronchoalveolar cell carcinoma. EHE can arise from many organs, including lungs, liver, bone, and soft tissue, simultaneously or sequentially. The distinction between multicentric primary tumor and metastasis may be difficult. The most characteristic feature of pulmonary EHE on chest imaging studies is the presence of multiple perivascular nodules with well- or ill-defined margins in both lungs. There is currently no standard treatment for EHE because of its rarity.

Pulmonary/Pleural Synovial Sarcoma (PPSS) in a Patient With Spontaneous Pneumothorax

B. Zhao. Department of Pathology and Laboratory Medicine McGovern Medical School at UTHealth at Houston, Texas.

A 25-year-old woman with a history of recurrent spontaneous pneumothorax at age 12 and 13 underwent video-assisted thoracoscopic pleurodesis and left upper lobe wedge resection. In May 2018 she suffered sudden-onset left-side chest pain and was suspected to have another pneumothorax. A 7-cm cavity mass was found in the left upper lobe on imaging. A left thoracotomy and lobectomy were performed. Gross examination revealed a 7.0 × 6.5 × 5.0 cavity lesion filled with blood, and the pleura was irregular with fibrotic adhesion and disruptions. Sections of the resected lung showed a high-grade spindle cell malignancy involving the lung parenchyma and pleura. Much of the tumor was necrotic and showed intratumoral hemorrhage with intratumoral hematoma. Immunohistochemical stains showed a nonspecific immunophenotype, with patchy positivity for EMA and CK7. The spindle cells were negative for endothelial markers, excluding a vascular neoplasm. Further investigation revealed rearrangement of the *SS18* gene region by fluorescence in situ hybridization, confirming a diagnosis of monophasic synovial sarcoma. PPSS is extremely rare, accounting for <0.5% of all lung tumors. A diagnosis of PPSS is difficult for clinicians and pathologists because of the rare nature of the tumor. The morphology, immunostaining properties, cytogenetic features, and management strategy of PPSS are similar to those of soft tissue synovial sarcoma.